9-1998

An Examination of Information Technology Valuation Models for the Air Force

Todd A. Peachey

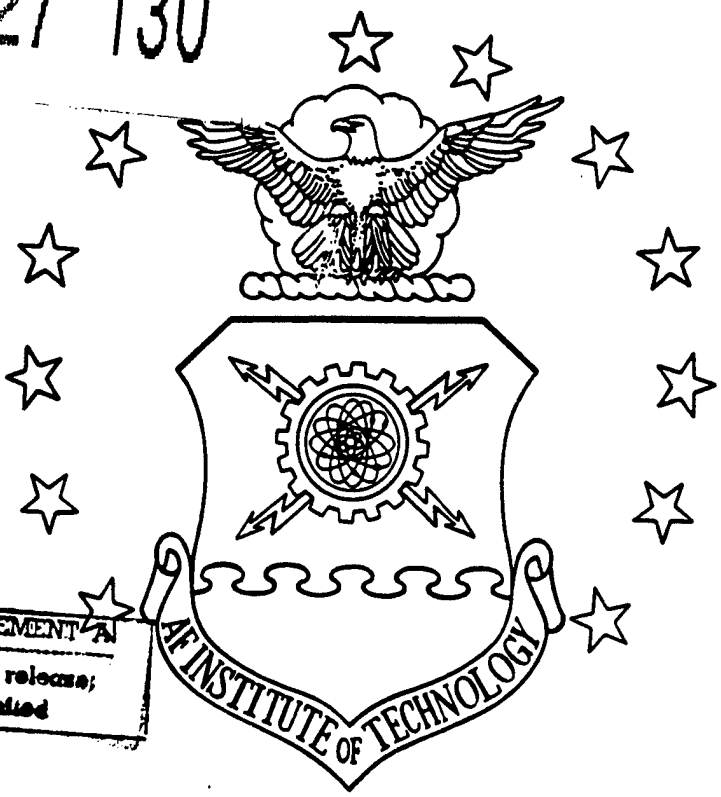

A Variable-Complexity Modeling Approach to Scramjet Fuel Injection Array Design Optimization

THESIS

Michael D. Payne, B.S.
Captain, USAF

AFIT/GOR/ENS/98M-18

DEPARTMENT OF THE AIR FORCE
AIR UNIVERSITY
AIR FORCE INSTITUTE OF TECHNOLOGY

Wright-Patterson Air Force Base, Ohio

AFIT/GOR/ENS/98M-18

A Variable-Complexity Modeling Approach to Scramjet Fuel Injection Array Design Optimization

THESIS

Michael D. Payne, B.S.
Captain, USAF

AFIT/GOR/ENS/98M-18

AFIT/GOR/ENS/98M-18

A Variable-Complexity Modeling Approach to Scramjet Fuel Injection Array Design Optimization

THESIS

Presented to the Faculty of the Graduate School of Engineering of the Air Force Institute of Technology Air University In Partial Fulfillment for the Degree of

Master of Science

Michael D. Payne, B.S.

Captain, USAF

Air Force Institute of Technology

Wright-Patterson AFB, Ohio

March, 1998

High Speed Systems Development Branch, Propulsion Sciences and Advanced Concepts Division, Propulsion Directorate, Air Force Research Laboratory, Wright-Patterson AFB, OH (AFRL/PRSS)

AFIT/GOR/ENS/98M-18

A Variable-Complexity Modeling Approach to Scramjet Fuel Injection Array Design Optimization

Michael D. Payne, B.S.

Captain, USAF

Approved:

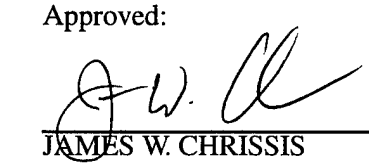

JAMES W. CHRISSIS
Associate Professor of Operations Research
Department of Operational Sciences
Advisor

17 Feb 98
Date

EDWARD A. POHL, Maj, USAF
Assistant Professor of Systems and Aerospace Engineering
Department of Aeronautical and Astronautical Engineering
Advisor

17 Feb '98
Date

RODNEY D.W. BOWERSOX
Assistant Professor of Aerospace Engineering
University of Alabama
Reader

17 Feb '98
Date

Dedication

This work is dedicated to my father, David Harold Payne. His field is neither Operations Research nor Aerospace Engineering, but rather the art of helping young adults shape their futures. Many have benefitted from his unique ability to distill the most fundamental aspects of a problem from the enormous complexities of life. For thirty years, he has helped others clarify their objectives and honestly assess the constraints imposed, sometimes most cruelly, by the human condition. His search for solutions was tireless; he was neither hindered by the difficulty of a problem nor dissuaded by the impossibility of providing "optimal" solutions to those he helped through life. I hope I've brought a small piece of his gift to this research. Your influence is with me always, Dad, and for that I am ever grateful.

Michael David Payne

Acknowledgments

This work would not have been possible without the enormous contributions of my research committee. My reader, Dr. Rodney Bowersox, garnered the necessary support for this effort, and shared his considerable knowledge and experience throughout the investigation. My advisors, Dr. James Chrissis and Major Edward Pohl, provided a wealth of expertise to draw upon, particularly with regard to the application of operations research methods to engineering design. They allowed me great freedom to conduct this research, and in so doing made this learning experience complete. I am also indebted to Lieutenant Colonel Glenn Bailey who, though not on my committee, generously lent his response surface expertise to this research. Special thanks go to my sponsors at the Air Force Research Laboratory, who provided tremendous support to this effort. Dr. Raymond Fuller's guidance and expertise were essential to success, particularly in formulating the design problem and assessing design performance. Dr. Mark Gruber's commitment to this research provided much needed stability in a turbulent process; his direction and insight improved the quality of the investigation immensely. To my wife, Melissa, I express my deepest gratitude. In a difficult year, her patience, love, and support made all the difference.

Table Of Contents

List Of Figures

List Of Tables

Abstract

The analysis of fuel-air mixing in a scramjet is often accomplished either with computational fluid dynamics (CFD) algorithms or through experimental research. These approaches, while accurate and reliable, are extremely expensive and thus not well-suited for use with conventional design optimization methods. In this investigation, Variable-Complexity Modeling (VCM) is used to significantly reduce the number of complex, expensive analyses required to optimize the design of a scramjet fuel injection array. A design problem formulation for a lateral transverse injection array is developed and a VCM approach to design optimization is conducted in two stages. Initially, a simplified analysis model is used to provide relatively inexpensive predictions of design fuel-air mixing characteristics. A parametric analysis is conducted to explore the design region, and a preliminary optimal design is found using both Sequential Quadratic Programming and a Genetic Algorithm. In the second stage, response surface methodology is supplemented with preliminary stage information to minimize the number of expensive analyses required to finalize the design. It is shown that only 25 design evaluations are required to develop a near-optimal design.

A Variable-Complexity Modeling Approach to Scramjet Fuel Injection Array Design Optimization

Chapter 1 - Introduction

1.1 Background

In 1903, the Wright brothers made their historic first flight into the skies at Kittyhawk. Since then, aircraft have been designed and built with an unwavering purpose: to fly higher and faster than ever before. Less than a century later, our sights are set on the ultimate goal of achieving flight at any speed and altitude [1] . This quest will be realized by an aircraft capable of taking off from a conventional runway, accelerating to hypersonic speeds, and coasting into low-earth orbit.

Hypersonic speeds and transatmospheric flight are currently achievable, but not with an air-breathing propulsion system. The SR-71, capable of flight speeds exceeding Mach 3, is the fastest known air-breathing aircraft [2] . Only rocket propulsion systems are currently capable of reaching hypersonic speeds. Rockets, however, must carry their own oxidizer for combustion, and therefore are a costly and inefficient means of transporting payload through the atmosphere. An air-breathing system does not suffer a comparable weight penalty, as the available oxygen in the atmosphere is used for oxidation. Table 1 illustrates the contrast in typical takeoff weight fractions (**TWF**) for rocket and aircraft systems [1] .

Table 1. Takeoff Weight Fractions

TWF	**Rocket**	**Aircraft**
Oxygen	65 %	0 %
Fuel	24 %	30 %
Empty	7 %	55 %
Payload	4 %	15 %

The severe weight penalty imposed by the oxidizer results in reduced rocket payload and empty weight fractions. Large, heavy vehicles are required to compensate for the small rocket payload fraction. Reduced empty weight leaves less weight available for rocket structures, controls, and instrumentation. This significantly reduces margins for error and results in less durable, more expensive vehicles [1] . In contrast, aircraft are proportionately smaller and more cost-effective since a larger weight fraction is available for payload. An aircraft is also more durable, since more weight is available for the structure and systems. In addition, exceedingly complex and expensive rocket launch facilities are not required for an air-breathing aircraft. These aircraft will operate from traditional runways [1] , thereby significantly reducing the support costs associated with rocket launches. Clearly, hypersonic air-breathing propulsion offers several advantages over current rocket technology for transatmospheric flight. The promise of these benefits has fueled the growth of hypersonic research, and renewed the quest to fly higher and faster.

1.1.1 Scramjet Engines

Transatmospheric flight will not be realized by traditional turbojet and ramjet engines, which are incapable of reaching hypersonic speeds. Conventional engines, including those that operate at supersonic flight conditions, decelerate the incoming airflow to provide subsonic flow to the combustor. Relatively low-speed flows are desirable in a combustor to allow sufficient time for complete fuel-air mixing and efficient combustion.

As the entering air is decelerated by the engine inlet, the relative velocity of the air, and thus its kinetic energy, decreases. Energy conservation requires that a decrease in kinetic energy be accompanied by a corresponding increase in the internal energy of the flow. This conversion is manifested as an increase in the pressure, density, and temperature of the airstream. As the flight Mach number increases, the amount of kinetic energy converted to internal energy also increases.

For flight Mach numbers greater than about 6, the temperature increase caused by deceleration of the flow to subsonic speeds is sufficient to incinerate most known structural materials. In addition, such temperatures cause dissociation of the combustion constituents, and a subsequent loss of a large portion of the chemical energy required for thrust generation [1] .

Therefore, the conventional approach of decelerating the flow to subsonic conditions must be abandoned if flight Mach numbers above 6 are to be achieved. It is possible to avoid these excessively high temperatures by limiting the flow deceleration in the engine inlet. As a result, the flow entering the combustor remains supersonic and combustion must occur under supersonic flow conditions. An air-breathing engine that employs supersonic combustion is referred to as a *s*upersonic *c*ombustion *ramjet*, or a *scramjet* [1] . The Air Force Research Laboratory (AFRL/PRSS) is currently conducting research to develop a scramjet engine. Figure 1 shows a scramjet combustor in the AFRL/PRSS research facility.

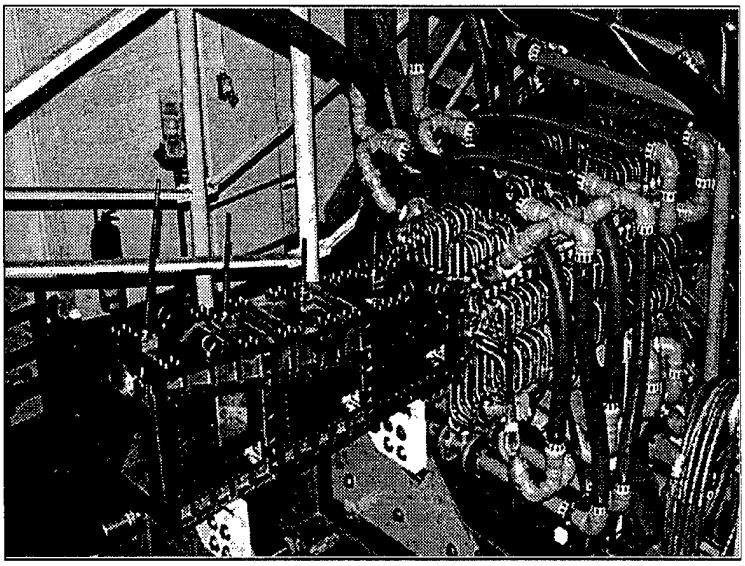

Figure 1. AFRL/PRSS Scramjet Combustor Development Facility

1.1.2 Fuel Injection

Achieving stable and efficient combustion under supersonic conditions presents several challenges, most notably fuel injection. In a supersonic combustor, the residence time of any fluid particle is on the order of only 10^{-3} seconds. Thus, sufficient penetration, mixing of the fuel and air, and combustion must occur over an extremely short time period [3] . The problem is further complicated by total pressure losses that are incurred when penetration and mixing rates are improved. Total pressure losses translate directly to severe reductions in combustor efficiency [1] .

There are two primary methods used to inject gaseous fuel into a supersonic airflow: *transverse* and *swept-ramp* injection. Transverse injection consists of a wall-flush port through which a gas is injected directly into the supersonic freestream. Figure 2 is an illustration of transverse injection with a single jet [4] . The transverse injection scheme is often enhanced by injecting the

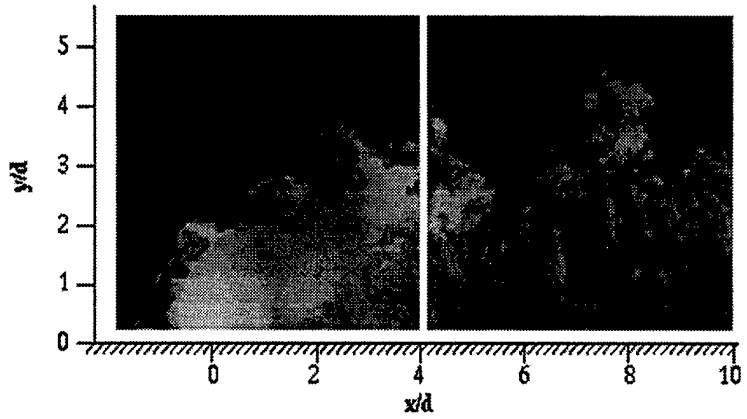

Figure 2. Transverse Injection

gas at angles between normal and parallel to the freestream. Intuitively, normal injection provides maximum near-field penetration but also maximizes pressure losses, and thus decreases thrust po-

tential. Parallel injection can enhance thrust due to additional momentum flux from the fuel jet, but does not provide sufficient penetration and mixing within the required residence time [5] .

Swept-ramp injection is the injection of a gas from the downstream face of swept ramps placed in the freestream. The presence of swept ramps causes spillage of high pressure air off and around the inclined compression surfaces, thereby generating vorticity to enhance mixing [6] . A typical swept-ramp injector is illustrated in Figure 3. This method appears to yield significant improve-

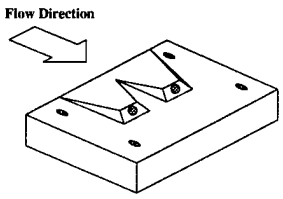

Figure 3. Swept-Ramp Injectors

ments in far-field mixing, but also contributes significantly to pressure losses in the combustor. In addition, ramps placed in the freestream may require active cooling mechanisms to prevent incineration at high flight Mach numbers. While transverse and swept-ramp injection are both considered viable candidates for future combustor designs, an investigation of both methods is beyond the scope of this study. Due to the availability of analysis software [7] , this investigation focuses exclusively on transverse injection.

1.1.3 Scramjet Combustor Analysis

As with many engineering design problems, scramjet combustor analysis is often accomplished via computational algorithms. Computational fluid dynamics (CFD) methods currently provide results that agree closely with the available experimental data for non-reacting flows. However, CFD analysis is extremely time-consuming, even on the most powerful computers. The cost of

executing a three-dimensional CFD simulation for scramjet combustor analysis is estimated to be on the order of $10,000 per run [7] . Such extreme computational intensity is a severe impediment to research aimed at enhancing fuel injection efficiency. Moreover, it is not feasible to use CFD in conjunction with conventional mathematical programming methods, which would require hundreds of CFD runs in the course of determining an optimal fuel injection design.

Billig and Schetz [7] have developed a simplified analysis method, *JETPEN,* to predict the major properties and features of a transverse injection flowfield at a reasonable computational cost. The results obtained with *JETPEN* were compared to the experimental data in [5] , [8] , and [9] , and found to be as accurate as results obtained from the most sophisticated CFD codes [7] . The *JETPEN* code is, therefore, capable of providing reliable design assessments rapidly enough to make integration with a conventional optimization approach computationally feasible.

1.2 Purpose of the Research

Scramjet fuel injection array design has not been previously studied in the context of a design optimization problem. As such, this investigation begins with a formulation of the design problem and a description of the design evaluation method. A fuel injection plate, illustrated in Figure 4, will

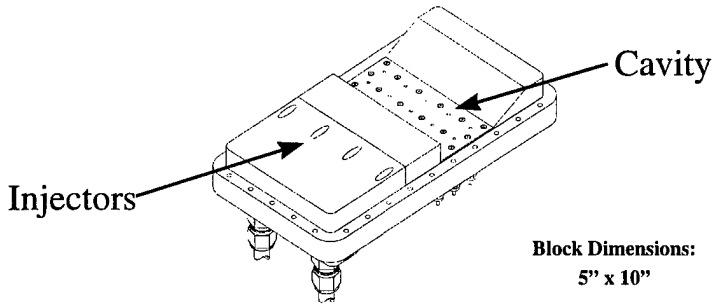

Figure 4. AFRL/PRSS Fuel Injection Array

be designed for the AFRL/PRSS combustor shown in Figure 1. The fuel injection array consists of a lateral row of circular, wall-flush injector ports that will be designed to optimize fuel-air mixing. The purpose of this research is to develop a Variable-Complexity Modeling (VCM) approach to minimize the cost of optimizing the scramjet fuel injection array design.

VCM is a two-stage approach designed to minimize computational effort by reducing the number of complex analyses required to locate an optimal design. The VCM approach is illustrated in Figure 5. Initially, a simplified analysis method is used in conjunction with conventional optimiza-

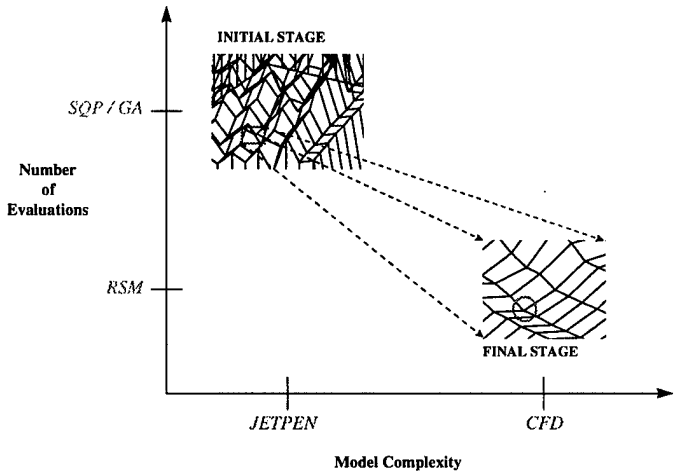

Figure 5. Variable-Complexity Modeling Approach

tion techniques to quickly explore the design space and develop a preliminary optimal design. The size and complexity of the problem are reduced in this stage by screening out regions of the design space that obviously do not contain the optimal design. In this investigation, *JETPEN* is used as the simplified design assessment tool and two optimization methods, Sequential Quadratic Programming and a Genetic Algorithm, are used to develop the preliminary optimal design. In the second stage of VCM, complex analysis methods are used in conjunction with response surface methodol-

ogy to verify the preliminary analysis and finalize the design. However, since *JETPEN* is capable of providing accurate and reliable design assessments [7] , it is used in this investigation to demonstrate the final-stage VCM approach and thus provide a basis for future research; time limitations precluded the use of CFD and/or experimental analysis methods in this study. This investigation concludes with recommendations for future research.

Chapter 2 - Literature Review

2.1 Overview

The literature relevant to this effort is conveniently divided into two categories. First, literature related to the study of transverse injection is presented. Emphasis is placed on developments contributing to an understanding of the fundamental flow physics, as well as on the progress of mixing and penetration enhancement. Second, relevant optimization literature is reviewed from a historical perspective. The focus is not to present a comprehensive review of optimization, but rather a survey of the algorithms and heuristics commonly employed to optimize computationally-intensive engineering design problems. This review concludes with an introduction to Variable-Complexity Modeling (VCM)–a relatively new technique developed to minimize the cost of optimization.

2.2 Transverse Injection

Transverse injection is the injection of a gas from a wall-flush port into a crossflow. The open literature is abundant with studies of transverse injection and the factors that influence the fuel-air mixing performance. Several factors are considered critical to the penetration, mixing, and pressure loss characteristics of a transverse injection configuration. These include the dynamic pressure of the injectant, the angle of injection, and the number and arrangement of injectors employed [3] . Each of these factors is addressed in detail.

2.2.1 Injectant Dynamic Pressure

The ratio of injectant dynamic pressure to freestream dynamic pressure ($\overline{q}$) significantly affects mixing and penetration of the jet [10] . Consider first the effect of $\overline{q}$ on mixing rate. Increasing $\overline{q}$ may be achieved either by increasing the velocity or density of the injectant stream. If the velocity is increased, there is less time available for the injectant to mix with the freestream, and mixing rate decreases. Similarly, increasing the density results in an injectant stream that is more resistant to

mixing with the main flow, and thus more time is required for mixing. It is therefore apparent that mixing rate is inversely proportional to $\overline{q}$ [6] . This is true for near-field mixing [3] , but far-field mixing is relatively unaffected by $\overline{q}$ [8] . In the far-field, mixing is largely dominated by small-scale turbulence effects [11] .

In contrast, penetration is improved by increasing $\overline{q}$, as a more dense or more rapidly moving stream forces the Mach disk further into the crossflow [5] . If the injectant stream is supersonic, it will penetrate the main flow further than a sonic injectant stream. However, increased penetration requires that the jet be turned more sharply, which generates increased pressure losses in the flow [10] .

2.2.2 Injection Angle

Normal injection angles can produce reasonable penetration and mixing. This configuration, however, requires the freestream to turn the injectant flow through a 90^o angle. This turning, coupled with the barrier presented to the main flow by the jet, causes significant total pressure losses. In contrast, fuel injected parallel to the main flow can contribute to thrust generation. However, parallel injection produces no penetration and relies strictly on shearing effects for mixing [5] . Shearing results in extremely slow mixing rates, and thus requires a prohibitively long combustor to complete the process [1] .

Several attempts have been made to balance the advantages and disadvantages of these extremes. McClinton [9] investigated circular jets at $30^o, 45^o, 60^o$, and 90^o downstream angles and concluded that decreasing the angle increased penetration and mixing and reduced total pressure losses. Mays, Thomas, and Schetz [5] studied low-angle injection and found that penetration depended strongly on $\overline{q}$. They demonstrated that a jet injected at 15^o attained the same penetration as a normally injected jet, given similar dynamic pressure ratios. In addition, they showed that de-

creasing the injection angle improves the near-field mixing rate, but has little effect in the far-field. Continued attempts to decrease the angle, however, eventually produce results approaching the parallel injection scheme. No studies were found to indicate the limit of low-angle injection.

2.2.3 Injection Array

The effects of multiple injectors have also been investigated. Rogers [8] injected hydrogen into a Mach 4 crossflow with a lateral row of injectors at two distinct spacing intervals: 6.25 and 12.5 jet diameters. Interaction of the jets was found to be minimal for the wider array, and thus the results were comparable to a single jet configuration. The narrower array produced significant jet interaction, which resulted in 30% greater total pressure losses and decreased mixing efficiency. By staging two injectors in the axial direction, Hollo *et al.* [11] produced a significant improvement in initial mixing rate over that of a single injector, and concluded that injector configuration is critical to near-field mixing. Furthermore, it is noted that mixing is most effectively enhanced through vortex generation and jet-vortex interaction, which unfortunately lead to increased total pressure losses.

2.3 Optimization

A review of the literature produced scant evidence of scramjet combustor design optimization. This is not surprising, as most of the efforts to date have focused on understanding and modeling the complex physical phenomena involved. However, scramjet research is progressing rapidly: NASA's Hyper-X program is scheduled to fly a hypersonic aircraft powered by a hydrogen-fueled scramjet engine to Mach 7 in early 1999 [2] .

As basic research is augmented with flight-test data, analytical and CFD modeling will become increasingly reliable. Once sufficient understanding of scramjet combustion is achieved, a portion of the research effort will shift to optimizing the design. This has certainly been true of other aerospace disciplines, most notably controls, structures, and more recently, aerodynamics. Opti-

mization techniques pioneered in these fields provide an appropriate point of departure for the study of scramjet optimization.

2.3.1 Mathematical Programming

Early work in engineering design optimization relied primarily on well-established mathematical programming (MP) techniques. These methods solve the general nonlinear programming problem by generating a sequence of design points $(x_0, x_1, x_2, ...)$ using the iterative scheme [12] :

$$\mathbf{x}_{k+1} \leftarrow \mathbf{x}_k + r_k \mathbf{d}_k$$

where k designates the current iteration, $\mathbf{x}_k$ is the design vector at the kth iteration, $\mathbf{d}_k$ is the search direction, and r_k is the step-size taken along the search direction. A framework for the general MP algorithm can be described as follows [12] :

Step 1: Select an initial design, $\mathbf{x}_o$; set $k \leftarrow 0$

Step 2: Determine the search direction, $\mathbf{d}_k$

Step 3: Determine the step-size, r_k

Step 4: Set $\mathbf{x}_{k+1} \leftarrow \mathbf{x}_k + r_k \mathbf{d}_k$

Step 5: Test for convergence

Step 6: If stopping criteria is not met, set $k \leftarrow k + 1$ and go to Step 2.

MP algorithms are distinguished by the strategies selected to determine $\mathbf{d}_k$ and r_k in Steps 2 and 3. Due to their size and complexity, practical engineering design problems require algorithms that are highly efficient and globally convergent (converge from any initial starting design). One of the most successfully applied MP techniques is Sequential (or Recursive) Quadratic Programming (SQP), which has been widely used to solve a variety of problems, including large-scale structural optimization problems. In this method the search direction is determined by solving a quadratic

subproblem at each iteration [13] :

$$\text{minimize} \qquad Q = \mathbf{d}^T \cdot \boldsymbol{\nabla}\mathbf{f} + \tfrac{1}{2}\mathbf{d}^T \cdot \mathbf{H}(\mathbf{x}, \boldsymbol{\lambda}) \cdot \mathbf{d}$$

subject to:

$$g_j(\mathbf{x}) + \mathbf{d}^T \cdot \nabla g_j(\mathbf{x}) \leq 0 \quad j = 1, ..., m$$

where $\mathbf{d}$ is the search direction, $\boldsymbol{\nabla}\mathbf{f}$ is the gradient of the original objective function, $\boldsymbol{\lambda}$ is a vector of Lagrange multipliers, $\mathbf{H}$ is an approximation of the Hessian of the Lagrange function ($\nabla^2 L$), and m is the total number of constraints. It can be shown that this subproblem is identical to a Newton-Raphson solution of the Kuhn-Tucker necessary conditions for the original problem [14] . This method has been shown to be globally convergent and to converge superlinearly near the solution point [15] .

Thanedar *et al.* [14] applied several variations of SQP to seventeen moderately-sized structural design problems. SQP efficiency was heavily influenced by the effective use of a potential constraint strategy. This potential constraint strategy is based on the observation that, for many problems, only a small number of the total constraints are active at the optimal design point. Thus, the number of constraint gradient evaluations is significantly reduced by selecting an appropriate subset of the constraints at each iteration [14] . This is particularly important for problems that rely on expensive finite element or CFD analyses to obtain gradient information. A thorough discussion of potential constraint strategies can be found in [16] .

Although SQP methods are globally convergent, they generally perform poorly on problems that possess multiple local optima. Belegundu and Arora [15] applied a variant of SQP, known as Pshenichny's method, to structural design problems known to possess a global optimum, as well as several local optima. The small step-sizes inherent to Pshenichny's method (and many other SQP variants) caused consistent convergence to the local optimum nearest the starting design. In fact, the algorithm was effective only when the starting design was known to be in the region of the global

optimum. This constitutes a major disadvantage of MP methods, since multiple local optima are common in engineering design problems and the location of the globally optimal region is rarely known *a priori*.

Belegundu and Arora suggest that a hybrid method could be used to overcome this problem. Initially, the globally optimal region can be located with a method using a large step-size. Pshenichny's method can then be used to quickly converge to the minimum [15] . Other MP-based global optimization techniques include the stochastic approach of Kan and Timmer [17] and the tunneling method of Levy and Gomez [18] . In the stochastic approach, the objective function is sampled at a fixed number of points in the design space. Local searches are performed in promising regions, and the process is repeated to increase the likelihood of locating the global optimum. The tunneling method also involves repeated local searches. However, each time a local optimum is found, the method seeks another design point with an equivalent function value. If such a point is found, a local search is started from that point to locate an improved local optimum. If no such point exists, then the current local optimum is also the global optimum.

Although global optimization is currently an area of intensive research, the stochastic and tunneling methods highlight the difficulties yet to be overcome. Global stochastic methods often involve a large number of function evaluations to achieve a high probability of locating the global optimum. Since most practical engineering design problems involve complex design evaluation procedures such as CFD, global stochastic methods are usually extremely expensive. The tunneling method is significantly more efficient, but currently requires an explicit statement of the objective function. For most practical design problems, system performance can only be expressed as an implicit function of the design variables.

2.3.2 Heuristics

Heuristic methods have been explored as alternatives to MP for locating the global optimum in problems possessing multiple local optima. In determining the search direction $\mathbf{d}_k$, MP methods only allow directions that result in improvement of the objection function. If an MP algorithm encounters a local maximum, it cannot escape since all directions away from the local maximum, within a specified neighborhood, result in an objective function decrease. In essence, the MP method cannot move downhill to climb an adjacent, higher peak. Heuristic methods are designed to accept all uphill moves, and also to allow downhill moves in specified circumstances. This strategy allows the possibility of escaping from local optima, and thereby increases the probability of locating the global optimum.

Simulated Annealing (SA) is a heuristic method based on the physical process of *annealing*, a two-step thermal process for obtaining low (minimal) energy states of a solid in a heated bath. The solid is first melted by increasing the temperature of the bath to some maximum value. The temperature is then carefully decreased until the particles are arranged in a highly-structured lattice. To achieve this minimum energy state, the maximum temperature must be sufficiently high, and the cooling rate must be sufficiently slow. In 1953, Metropolis developed the following algorithm to simulate the annealing process (k is Boltzmann's constant and T is the temperature of the heated bath) [13] :

Step 1: Perturb the system energy from the current state, E_1, to a new state, E_2

Step 2: If the energy of the system drops ($E_2 < E_1$), accept E_2

Step 3: If the energy of the system rises ($E_2 > E_1$), accept E_2 with probability:

$$P = \exp\left[\frac{-(E_2 - E_1)}{kT}\right]$$

The simulated annealing optimization algorithm is analogous to the Metropolis algorithm. In SA, the energy of the system in state i (E_i) is represented by the objective function value at a

particular design point. Step 3 is the provision that allows deterioration of the objective function and permits SA algorithms to escape local optima [19] .

Aly *et al.* [20] recently compared SA to an SQP method in designing the shape of a High Speed Civil Transport (HSCT). This problem is particularly relevant for two reasons. First, a CFD solver was used, and thus objective function and constraint evaluations were expensive. Second, the problem contained several local minima. As expected, the SQP method often converged to local minima, while the SA algorithm located the global minimum in each of the three design problems. Both the MP and SA algorithms required a large number of CFD evaluations, and thus were extremely expensive from a computational standpoint.

Ogot *et al.* [21] also conducted a comparison of SA and SQP on three supersonic flow design problems. In this case, the existence of strong shock waves in the flow combined with CFD discretization errors to produce a non-smooth, noisy objective function. This presented severe problems for the SQP algorithm, which was unable to locate the global minimum in several instances. The SA method was unaffected by discontinuities and noise, but also proved to be inefficient. Although several promising modifications to the basic heuristic were explored, the SA consistently required approximately 150 to 200 CFD runs to converge.

Genetic Algorithms (GA) have also been used extensively in structural and aerodynamic design. A GA is an intelligent random search method based on Darwin's theory of survival of the fittest [22] . In a GA, multiple alternate solutions to the optimization problem represent individuals in a natural population. Individuals are formed by encoding the decision variables and concatenating them to yield a single string. This chromosomal structure facilitates the simulation of evolution through natural selection, mating, crossover, and mutation processes. The fitness of each individual in the population is represented by the objective function value corresponding to each potential

solution. Thus, a solution to the optimization problem is found by using the evolutionary processes to maximize the fitness of the population.

As with SA, GAs are often successful in locating global optima, but are also computationally expensive. Hajela [23] tested a GA on three structural design problems known to exhibit non-convex and/or disjointed design spaces. In all cases, the GA located the optimal design where MP techniques failed, but the required number of function evaluations was large. Similarly, Deb [24] compared a GA with both an MP method and a random search method. As expected, the GA was slightly more expensive than the MP method and significantly cheaper than the random search.

Obayashi and Tsukahara [25] , Anderson [26] , and Foster and Dulikravich [27] applied GAs to aerodynamic shape design. In each case, the GA proved essential for successfully locating global optima. Again, however, the number of required function evaluations proved to be quite large in all cases.

Excessive computational cost in these GA studies is directly related to the need for large populations, which are required to maintain diversity in the search and prevent premature convergence to a sub-optimal result. Population sizes between 30 and 200 are typical, and a function evaluation is required for every individual. Krishnakumar [28] reports impressive results with a micro-genetic algorithm (μGA) which maintains a very small population of 5 individuals. The μGA was compared to a conventional GA and found to reduce the required number of function evaluations by a factor of four. In this respect, the μGA represents a significant improvement over conventional SA and GA algorithms, and is thus a viable candidate for expensive optimization problems.

2.3.3 Response Surface Methodology

Response Surface Methodology (RSM) can be exploited to significantly reduce computational effort in the optimization process, and is often the only feasible approach to CFD-based design

problems. A response surface is a polynomial approximation to the actual response of a complex system. The model used for approximation is [29] :

$$\mathbf{y} = Z\boldsymbol{\beta} + \varepsilon$$

where $\mathbf{y}$ is a vector of responses, Z is an experimental design matrix, $\boldsymbol{\beta}$ is a vector of unknown polynomial coefficients, and ε is the error. Experiments are conducted to measure the system response at prescribed points in the design space, and the method of least squares [29] :

$$\widehat{\boldsymbol{\beta}} = \left(Z^T Z\right)^{-1} Z^T \mathbf{y}$$

is used to estimate the polynomial coefficients. In this context, an experiment is one complete execution of the design evaluation code. The resulting response surface:

$$\widehat{y} = \mathbf{z}\widehat{\boldsymbol{\beta}}$$

is typically a low-order polynomial that is easily optimized with a standard MP algorithm. Therefore, the computational intensity of the problem is determined not by the optimization method selected, but by the number of experiments required to construct the approximating polynomial.

The fundamental experimental design is a full-factorial design. To construct a second-order response surface using a full-factorial design, three levels of the n design variables are required to estimate the coefficients [29] . Thus, 3^n experiments are required. Full-factorial designs quickly lead to a large number of experiments as the number of design variables increases. For example, a problem containing only four design variables requires $3^4 = 81$ experiments.

The Central Composite Design (CCD) is a popular alternative to full-factorial designs. By augmenting a first-order design, which requires only 2^n experiments, a second-order response surface can be constructed using just $2^n + 2n + 1$ design points [29] . This reduces the required number of experiments for a four-variable problem from 81 to 25.

In some cases, CCDs may still be too expensive, and saturated experimental designs must be used to further reduce the number of experiments. Box and Draper [30] have developed minimum-

point second-order designs consisting of $\frac{1}{2}(n+1)(n+2)$ design points. For such a design, a four-variable problem requires just 15 experiments, compared with 81 and 25 for the full-factorial and CCD designs, respectively [31] . These designs contain no residual degrees-of-freedom to test for model inadequacy, and thus should be used only when cost constraints preclude the use of alternate designs.

Chen *et al.* [32] applied RSM to the design of an HSCT with two important results. First, the Flight Optimization System typically used in HSCT design produced noisy objective functions that often confounded MP optimizers. The response surface approximation yielded a smooth objective function and thus increased the chances of finding the optimal design. In addition, considerable computational efficiency was gained (85 *vs.* 531 experiments) without loss of accuracy through the judicious use of design of experiments. Unal *et al.* [31] used RSM to optimize a dual-fuel propulsion system problem with four design variables. The optimal design results were in close agreement with those obtained from a gradient-based optimizer, and were found with significantly less computational effort.

The most widely used experimental designs, variance-optimal designs, are constructed to minimize random error. As such, these designs do not directly address the systematic bias that arises from approximating a complex response with a low-order polynomial. Roux *et al.* [33] used variance-optimal designs for three structural problems of increasing complexity. In each case, the response surface was constructed several times over successively smaller regions of the design space using a variance-optimal design. Smaller subregions, which inherently reduce the systematic bias, were found to significantly increase the accuracy of the response surface approximation.

If the experimentation method is entirely deterministic, such as with *JETPEN* or CFD, there is no random error and hence the approximation problem is dominated by systematic bias [32] . Since systematic bias is of primary concern in such cases, minimum-bias designs should be used

in lieu of variance-optimal designs to construct response surfaces. Systematic bias results from approximating a system response with an insufficient model. If the fitted model is expressed as:

$$\widehat{y} = \mathbf{z}_1 \widehat{\beta}_1$$

then the true system response can be written as:

$$E(y) = \mathbf{z}_1 \beta_1 + \mathbf{z}_2 \beta_2$$

where β_1 and β_2 are the unknown coefficients of the true model, $\mathbf{z}_1$ contains the terms of the true response that are estimated in the fitted model, and $\mathbf{z}_2$ contains the higher-order terms not accounted for in the model that must be protected against in designing the experiment. Minimum-bias designs are developed by specifying $\mathbf{z}_1$ and $\mathbf{z}_2$ and minimizing the average squared bias over a region of interest [29] . This results in the following sufficient conditions for minimum-bias designs:

$$M_{11} = \mu_{11} \tag{1}$$

$$M_{12} = \mu_{12} \tag{2}$$

where the design moment matrices are given by:

$$M_{11} = \frac{Z_1^T Z_1}{N} \text{ and } M_{12} = \frac{Z_1^T Z_2}{N}$$

and the region moment matrices are:

$$\mu_{11} = K \int_R \mathbf{z}_1 \mathbf{z}_1^T d\mathbf{x} \text{ and } \mu_{12} = K \int_R \mathbf{z}_1 \mathbf{z}_2^T d\mathbf{x}.$$

In these expressions, R is the region of interest, K is the inverse of the region volume, and N is the total number of experimental observations.

Venter and Haftka [34] compare variance-optimal and minimum-bias designs for constructing response surface approximations in structural design problems where bias error is present. In these cases, the response surfaces constructed from minimum-bias designs were indeed found to be more accurate than those based on variance-optimal designs.

2.4 Variable-Complexity Modeling

Variable-Complexity Modeling (VCM) is an approach that utilizes both simple and complex system models to combine the best features of MP, heuristic, and RSM optimization methods. Initially, an MP or heuristic method is used with a simplified system model to quickly locate an approximate global optimum and screen out regions of the design space that obviously do not contain the optimal design. The complex system model is then run at experimental design points surrounding the approximate global optimum, and a response surface is constructed. In this manner, use of the expensive, complex model is held to an absolute minimum. Finally, the response surface is easily optimized using a conventional MP algorithm [35] .

VCM was successfully demonstrated by Gangadharan *et al.* [35] in the design of a beam using finite element analysis. An MP method with an active set strategy was used to locate the approximate global optimum. The design space was reduced from $3^5 = 243$ to 43 design points with a screening heuristic and a CCD. A response surface was constructed using the complex model, and an SQP algorithm was used for subsequent optimization. By constructing response surfaces from both the full and reduced designs, it was confirmed that using the simple model to reduce the design space significantly improved the accuracy of the response surface.

Similar variations of VCM have been applied to more complex aerodynamic and structural optimization problems. Hutchison *et al.* [36] used VCM to minimize gross weight by optimizing the aerodynamics of an HSCT wing. VCM significantly reduced computational intensity, yet preserved the interdisciplinary design influences typically masked by simplified approaches. Giunta *et al.* [37] used a similar problem to compare the accuracy of VCM with a sequential approximate optimization strategy. Differences in the optimal designs found by each method were negligible. Kaufman *et al.* [38] also used VCM to minimize HSCT wing structural weight, and found that

screening the design space with simplified models improved response surface accuracy by several orders of magnitude.

Variable-Complexity Modeling can be applied to scramjet fuel injection design optimization using the simplified jet penetration analysis, *JETPEN*, developed by Billig and Schetz [7] . *JETPEN* is based on the well-known case of an underexpanded jet discharged into a quiescent medium at a known back pressure [39] . Essentially, the effective back pressure in the supersonic crossflow is modeled with an average of the freestream static pressure and predictions for the pressure on inclined bodies based on Newtonian Impact Theory. The jet flowfield is treated as consisting of two distinct regions, shown in Figure 6 [39] , which are divided by a normal shock structure known as the *Mach disk*. From the injection port to the Mach disk, the jet is regarded as an intact entity. The jet

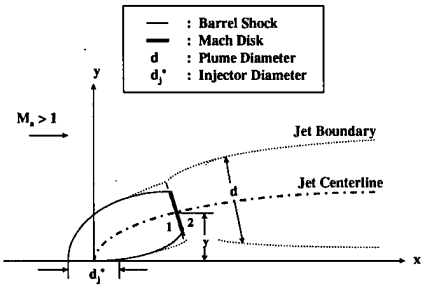

Figure 6. Transverse Injection Model

flow in this region is assumed isentropic, and mixing of the jet with the primary stream is neglected. Downstream of the Mach disk, the expanded jet flow is turned and mixed with the freestream. Turbulent mixing of the primary stream into the jet plume is modeled with mass continuity, streamwise momentum conservation, species conservation, and energy conservation equations, as well as an entrainment relation derived for high-speed flow [7] .

There are, however, at least two limitations to *JETPEN*. First, it does not provide total pressure loss data, which is critical in assessing overall combustor efficiency. This limitation essentially renders *JETPEN* a preliminary design tool, and highlights the need for CFD and/or experimental verification in the second stage of VCM. Second, *JETPEN* is not currently capable of examining staged injection configurations. Staged configurations have recently been used to produce an aerodynamic ramp effect, and thus represent a promising alternative to swept-ramp injection without the drawbacks of placing a physical ramp in the flow [40] . This limitation restricts the scope of this investigation to lateral fuel injection arrays.

2.5 Summary

Each of the optimization methods described in this review features characteristics designed to overcome specific difficulties that often arise in engineering design problems. However, all exhibit disadvantages that preclude their individual use for highly complex, computationally intensive problems. MP methods are globally convergent and highly efficient when near the design optimum, but generally perform poorly in the presence of noisy objective functions and/or multiple local optima. Heuristic methods do not require smooth objective functions and can often locate the global optimum, but at the cost of many objective function evaluations. RSM reduces the required number of experiments, but accuracy is sacrificed if the design space is not reduced to an appropriate subregion of interest.

In Variable-Complexity Modeling, MP, heuristics, and RSM are selectively combined to mitigate the respective shortcomings of each method. The objective of this investigation is to develop an appropriate combination of these methods and demonstrate a VCM approach to scramjet fuel injection array design.

Chapter 3 - Scramjet Fuel Injection Array Design

3.1 Overview

Fuel injection in a supersonic crossflow is still a challenging research problem, and thus little effort has been devoted to array design in the context of traditional optimization. The objective of this chapter is to develop and present both a formal statement of the lateral transverse fuel injection array design problem, and a method for evaluating design performance. Design problem formulation is the process of developing a mathematical model to describe the physical system of interest. The general form of this mathematical description is:

$$\text{minimize} \quad f(\mathbf{x})$$

$$\text{subject to:} \quad g_j(\mathbf{x}) \leq 0,\ j = 1, ..., m$$

where $\mathbf{x}$ is a vector of n design variables and m is the number of constraints on the system. The solution to this problem provides a design vector $\mathbf{x}$ that optimizes some measure of system performance $f(\mathbf{x})$ within prescribed limitations on system behavior, $g_j(\mathbf{x}), j = 1, ..., m$. Both minimization and maximization problems may be treated, since minimizing $f(\mathbf{x})$ is equivalent to maximizing $-f(\mathbf{x})$.

The development of a mathematical model for scramjet fuel injection array design is presented in five sections: a general description of the array configuration and detailed presentations of design variable selection, system constraint description, performance measure identification, and objective function development. The chapter concludes with a formal statement of the scramjet fuel injection array design problem and a description of the approach used to evaluate design performance.

3.2 Problem Description

The focus of this investigation is the design of a transverse fuel injection array for the AFRL/PRSS scramjet combustor shown in Figure 1. The general design concept, illustrated in Figure 7, consists of several (N) injectors arranged laterally across the width (l) of a rectangular combustor. The in-

jectors are circular, with diameter d_j^*, and are located at evenly-spaced intervals (w) in the array. In addition to the total combustor width (l), a non-fueled width (l_{nf}) is defined to account for cases in which manufacturing limitations prevent the installation of injectors within a prescribed distance from the combustor sidewalls. If no such restriction exists, then $l_{nf} = 0$.

The flow conditions are symmetric for this design, and thus the analysis is conducted only for the bottom half of the combustor ($h/2$). Although Figure 7 shows injectors at the bottom only, the final design will also have a second array to inject gas from the top of the combustor downward into the flow.

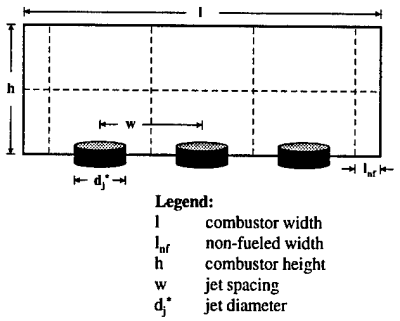

Figure 7. Injection Array Cross-Section

3.3 Design Variables

Formulation of the design problem begins with the selection of appropriate design variables. There are, in general, many potential design variables for this problem. However, the fuel injection array is to be designed to meet a specific mission requirement, and thus several potential variables must be considered fixed mission parameters. The mission requirement for this investigation, defined by AFRL/PRSS, is summarized by the parameters in Appendix A. These parameters include the fuel type, combustor size, and primary flow conditions in the combustor.

Given the mission parameters, the set of design variables for this problem is limited to the variables required to specify the injection array configuration and the jet flow conditions. Two additional values are sufficient to completely specify the lateral array design: the angle of fuel injection (δ_j) and the number of fuel injectors in the array (N). The injection angle is a direct *JETPEN* input parameter, and is therefore a convenient design variable. The number of injectors must be determined from Equation 22 (see Appendix B):

$$N = \frac{2l_f^2}{A_r Q \left(\frac{w}{d_j^*}\right)^2}$$

where

$$\begin{aligned} A_r &= \frac{l_f}{l} \\ Q &= \frac{4f\,\dot{m}_{tot}\,\sqrt{T_{T_j}}}{\pi c_j^* P_{T_j}} \end{aligned}$$

The fueled combustor width ($l_f = l - l_{nf}$) and the ratio of fueled-to-total width (A_r) are known parameters. The quantity Q (derived in Appendix B) is a function of the primary flow conditions, which are also known, and the jet flow conditions. Therefore, N may be calculated once the jet flow conditions and the non-dimensional spacing between the jets (w/d_j^*) are specified.

Since the injectant is assumed to behave as a perfect gas, only two independent intrinsic properties are required to completely specify the jet flow conditions. The jet total pressure (P_{T_j}) and total temperature (T_{T_j}) are convenient choices, as they are direct *JETPEN* input parameters. The non-dimensional jet spacing (w/d_j^*) is also a *JETPEN* input parameter, and is thus the final variable needed to specify the design. The four design variables (**z**) are listed in Table 2.

Table 2. Design Variables

z	Description	Units
δ_j	Injection Angle	deg
w/d_j^*	Jet Lateral Spacing	
P_{T_j}	Jet Total Pressure	$psia$
T_{T_j}	Jet Total Temperature	^oR

3.4 Constraints

3.4.1 Behavioral Constraints

The performance of a particular fuel injection array is measured by the flow behavior predicted by *JETPEN* for a given set of design variables. *JETPEN* predicts the flow behavior by solving the governing continuity, momentum, and energy equations with respect to the prescribed conditions. Thus, constraints on the behavior of the flow are implicit in *JETPEN* design evaluation. This implicit relationship is expressed in the following equality constraint:

$$\mathbf{x} = g\left[\delta_j, \frac{w}{d_j^*}, P_{T_j}, T_{T_j}\right]$$

where $\mathbf{x}$ is the vector of performance measures and g is a function that represents the governing equations imposed by *JETPEN*.

3.4.2 Side Constraints

Experimental data in [8] and [9] indicate that high-angle injection yields good penetration, but also results in a significant loss of total pressure in the primary stream. The magnitude of this loss increases as the injection angle increases. Since the total pressure loss is not accounted for in *JETPEN*, the injection angle is limited to a maximum of 70^o for this investigation.

Low-angle injection produces comparable far-field penetration and mixing without incurring the severe total pressure losses associated with high-angle injection. However, lower injection angles require longer injectors, which result in greater total pressure losses in the jet. At extremely low angles, it is both difficult and expensive to achieve a high total pressure at the injection point. Thus, the injection angle is limited to a minimum of 10^o, and the high- and low-angle injection limits are bounded by the constraint:

$$10^o \leq \delta_j \leq 70^o. \tag{3}$$

At each design iteration, the jet specific heat at constant pressure (c_{p_j}) and ratio of specific heats (γ_j) must be determined based on the proposed values of jet total pressure (P_{T_j}) and total temperature (T_{T_j}). These calculations are accomplished using polynomial approximations derived from tabular data provided by AFRL/PRSS. As a result, the ranges of P_{T_j} and T_{T_j} are limited by the range over which the polynomial approximations are valid. In addition, the jet total temperature must be high enough to ensure that the fuel (ethylene) is in a gaseous state during sonic injection. These restrictions dictate the following constraints on the jet flow conditions:

$$20\,psia \;\leq\; P_{T_j} \;\leq\; 650\,psia \tag{4}$$

$$850\,^{o}R \;\leq\; T_{T_j} \;\leq\; 1500\,^{o}R. \tag{5}$$

The non-dimensional spacing of jets within the combustor can be expressed by the following analytical expression (derived in Appendix B):

$$\frac{w}{d_j^*} = \frac{l_f}{\left[\frac{1}{2}NA_rQ\right]^{\frac{1}{2}}}. \tag{6}$$

Since the combustor dimensions and primary flow conditions are known, limits on the jet spacing can be determined from N and the constraints on P_{T_j} and T_{Tj}. The total number of jets in the injection array (N) is limited by the geometric restriction of fitting jets of finite diameter within a prescribed combustor width. For this investigation, the feasible range of N is constrained to:

$$3 \leq N \leq 10. \tag{7}$$

The bounds in constraints 4, 5, and 7 are thus easily combined with Equation 6 to produce the following jet spacing constraint:

$$2.25 \leq \frac{w}{d_j^*} \leq 22.10. \tag{8}$$

3.5 Performance Measures

The merit of a fuel injection array design is measured by the distance downstream of the injectors where sufficient fuel-air mixing has occurred and combustion may begin. Since the residence

time of the combustion constituents is extremely short in a scramjet combustor, mixing must occur as rapidly as possible. Thus, the optimal injection array design is the combination of δ_j, w/d_j^*, P_{T_j}, and T_{T_j} that produces sufficient fuel-air mixing over the shortest axial distance downstream of the injection point.

The mixing characteristics of a particular design are measured by the penetration of the jet into the primary stream, the expansion of the jet plumes, and the decay of fuel concentration in the jet. Three criteria are used to define the levels of these characteristics that constitute sufficient mixing. The axial distances where these criteria are satisfied thus comprise the performance measures for the design. For convenience, non-dimensional performance measures, obtained by normalizing all axial distances with respect to the combustor height, are used throughout this investigation; that is,

$$x_i^* = \frac{x_i}{h}$$

represents performance measure (i). For simplicity, the asterisk is hereafter omitted.

3.5.1 Jet Penetration

To maximize the time available for mixing, the jet must penetrate to the combustor centerline as rapidly as possible. Therefore, the first injection array performance measure is the axial distance required for centerline penetration. As illustrated in Figure 8, penetration of the jet is defined by

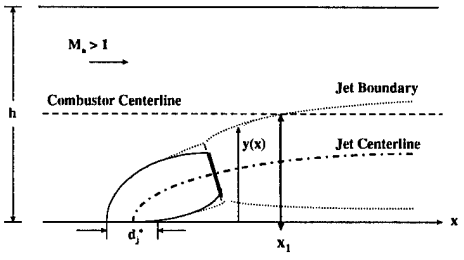

Figure 8. Jet Penetration

the height of the uppermost edge of the jet plume (y) at a given axial station. Thus, the jet reaches the centerline when:

$$y(x) \geq \frac{h}{2}$$

where h is the total combustor height. In *JETPEN*, variables with dimensions of length are normalized with respect to the injector diameter. Accordingly, the required penetration criterion is expressed as:

$$\frac{y(x)}{d_j^*} \geq \frac{h/2}{d_j^*} \tag{9}$$

to facilitate design evaluation with *JETPEN*. The first performance measure x_1 is the axial station where this penetration criterion is satisfied.

3.5.2 Plume Expansion

Mixing is also characterized by the rate of fuel plume expansion in the combustor. For a lateral array of injectors, the axial distance where adjacent fuel plumes merge is an indicator of the expansion rate. Figure 9 provides an overhead view of the injection array to illustrate plume expansion.

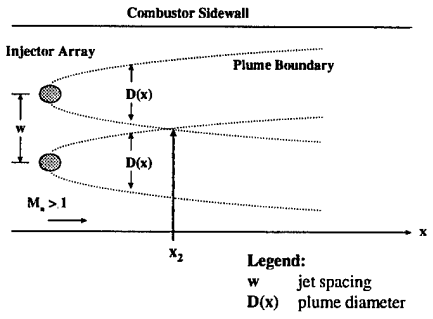

Figure 9. Plume Expansion

Adjacent plumes merge when the plume diameter (D) is greater than the spacing between injectors. Thus, the criterion for merging plumes is:

$$\frac{D(x)}{d_j^*} \geq \frac{w}{d_j^*}. \tag{10}$$

The second performance measure x_2 is the axial station where the plume expansion criterion is satisfied.

3.5.3 Fuel Concentration Decay

From the injection port to the Mach disk, the jet is composed entirely of fuel. Beyond the Mach disk, mixing progresses and the average concentration of fuel (α_{avg}) in the jet decreases as the primary stream is entrained. Figure 10 is a typical plot of the average fuel concentration decay.

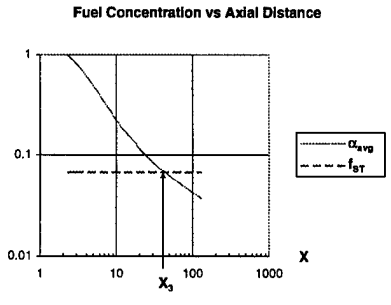

Figure 10. Fuel Concentration Decay

To maximize combustion efficiency, the average fuel concentration in the jet must decay to stoichiometric proportions. This criterion is expressed as:

$$\alpha_{avg}(x) \leq f_{ST}. \tag{11}$$

The third performance measure x_3 is the axial station where the fuel concentration decay criterion is satisfied.

3.6 Objective Function

Since mixing must occur as rapidly as possible, short axial distances, and thus smaller performance measures, indicate better designs. Consequently, the objective of fuel injection array design is to minimize some functional combination of the performance measures. This is expressed in an objective function as:

$$\text{minimize } f = f(\mathbf{x})$$

where $\mathbf{x} = [x_1\ x_2\ x_3]^T$ is the vector of the performance measures:

- $x_1 \equiv$ the axial distance to combustor centerline penetration
- $x_2 \equiv$ the axial distance to merge of adjacent jet plumes
- $x_3 \equiv$ the axial distance to stoichiometric fuel concentration decay.

Since this problem has not been previously studied, the most appropriate functional form of f is not known *a priori*. As such, six objective functions are used during the optimization process. Each of the three performance measures is used as an objective function separately, thus optimizing the design based on a single characteristic. Two additional objective functions are formed by using the 1- and 2-norms of the performance vector $\mathbf{x}$. Finally, a pareto-optimal solution is found by successively optimizing with respect to each performance measure. The value of the optimized performance measure is added as a constraint in each subsequent optimization.

Multiple objective functions are tested only in the first stage of VCM to maintain a feasible level of computational effort. Based on the preliminary analysis, a suitable objective function is recommended for use with more complex analysis methods.

3.7 Problem Statement

The design problem for a lateral scramjet fuel injection array is summarized as:

$$\text{minimize} \qquad f = f(\mathbf{x})$$

subject to:

$$\mathbf{x} = g\left[\delta_j, \frac{w}{d_j^*}, P_{T_j}, T_{T_j}\right]$$

$$10^o \leq \delta_j \leq 90^o$$

$$2.25 \leq \frac{w}{d_j^*} \leq 22.1$$

$$20\ psia \leq P_{T_j} \leq 650\ psia$$

$$850\ ^oR \leq T_{T_j} \leq 1500\ ^oR$$

$$3 \leq N \leq 10$$

The solution to this problem is the design vector, $\mathbf{z} = \left[\delta_j \;\; w/d_j^* \;\; P_{T_j} \;\; T_{T_j}\right]^T$, that optimizes some measure of fuel injection array performance, $f(\mathbf{x})$, within the prescribed limitations on system behavior.

3.8 Design Evaluation

The solution to the scramjet fuel injection design problem requires an evaluation of design performance at each iteration of the optimization process; that is, $\mathbf{x} = g[\mathbf{z}]$ must be computed for each proposed design vector $\mathbf{z}$. Design evaluation is accomplished with the jet penetration analysis software, *JETPEN*, developed by Billig and Schetz [7] . Two shell routines are used to integrate *JETPEN* with the optimization routines. The first shell routine is a pre-processor designed to accept a vector of design variables from an optimization program and prepare all required *JETPEN* input data. The second routine is a post-processor that collects *JETPEN* output data, evaluates the performance of the design, and returns an objective function value to the optimization software. An illustration of the integrated routines follows.

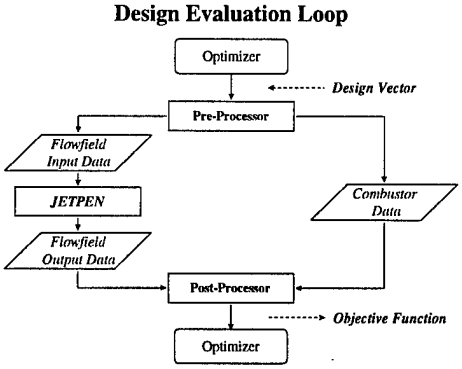

3.8.1 Pre-Processor

The pre-processor is designed to accomplish three primary functions. First, it collects all input data required for the design evaluation procedure. This data includes the design vector provided by the optimization program at each iteration, as well as the mission parameters specified by the user prior to optimization. Second, the pre-processor calculates both the dependent flow variables required for *JETPEN* input and the fuel injector design requirements necessary for performance evaluation. Two subroutines, described in detail, are used to perform these computations. Finally, the pre-processor generates an input file for *JETPEN* and a file containing the combustor design requirements to be used by the post-processor. The following diagram provides a graphical summary of this routine.

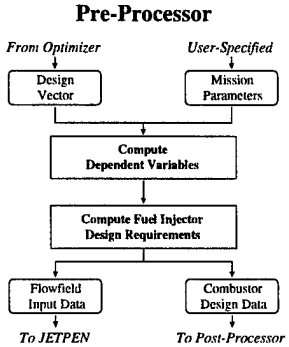

3.8.1.1 *Dependent Flow Variables*

The dependent flow variable subroutine is used to calculate the jet specific heat at constant pressure (c_{p_j}) and specific heat ratio (γ_j), which are required *JETPEN* input variables. These quantities are functions of two design variables and two parameters: the jet total pressure (P_{T_j}) and total temperature (T_{T_j}), and the molecular weight (w_j) and Mach number (M_j) of the injected fuel. This subroutine uses polynomial approximations to empirical data for ethylene provided by AFRL/PRSS to represent the functional relationship between these quantities.

Given P_{T_j}, T_{T_j}, w_j, and M_j, the following algorithm is used in conjunction with a simple bisection method to calculate corresponding values of c_{p_j} and γ_j:

Step 1: Compute $R = \frac{R_u}{w_j}$ where R_u is the universal gas constant

Step 2: Guess γ_j

Step 3: Convert to static conditions using isentropic relations:

$$P_j = \frac{P_{T_j}}{[1 + \frac{\gamma_j - 1}{2} M_j^2]^{\frac{\gamma_j}{\gamma_j - 1}}}$$

$$T_j = \frac{T_{T_j}}{[1 + \frac{\gamma_j - 1}{2} M_j^2]}$$

Step 4: Approximate $c_{p_j} = f(P_j, T_j)$ with AFRL/PRSS polynomials

Step 5: Calculate $\gamma_{j_n} = c_{p_j}/(c_{p_j} - R)$

Step 6: Compare γ_{j_n} to γ_j and iterate to convergence

3.8.1.2 *Fuel Injector Design Requirements*

The fuel injector design subroutine is used to calculate the injector diameter (d_j^*) and number of injectors (N) required by the design. Appendix B presents a detailed description of the analysis used in this subroutine to calculate these two quantities. The number of injectors is computed to evaluate the constraint given by Inequality 7:

$$3 \leq N \leq 10$$

using Equation 22 (derived in Appendix B):

$$N = \frac{2l_f^2}{A_r Q \left(\frac{w}{d_j^*}\right)^2}.$$

Subsequently, the injector diameter is computed to evaluate the penetration performance criterion, given by Inequality 9:

$$\frac{y(x)}{d_j^*} \geq \frac{h/2}{d_j^*}$$

using Equation 21 (derived in Appendix B):

$$d_j^* = \left[\frac{1}{2N} A_r Q\right]^{\frac{1}{2}}.$$

In these equations, l_f is the width of the combustor to be fueled by injectors and A_r is the ratio of fueled width to total width, given by $A_r = l_f \ / \ l$. The quantity Q (derived in Appendix B) is a function of the design variables and primary flow conditions.

3.8.2 Post-Processor

The post-processor is also designed to perform three functions. First, it collects the *JETPEN* output data and fuel injector design requirements needed for design evaluation. Second, a sub-routine evaluates the performance criteria, identifies the corresponding performance measures (**x**), and calculates the objective function for the given design. Finally, the post-processor generates an output file containing the performance information required by the optimization software. The following diagram illustrates this process.

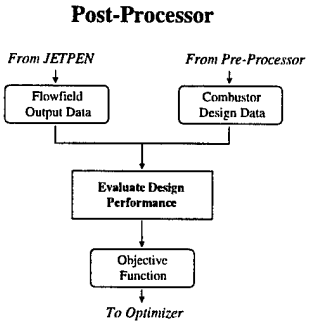

3.8.2.1 *Performance Analysis*

The performance analysis subroutine is used to evaluate the performance measures and compute the objective function. To do so, *JETPEN* is modified to produce an output file containing penetration data (y/d_j^*), plume spread data (D/d_j^*), and fuel concentration decay data (α_{avg}) at each axial station. This information is used to determine the axial stations at which the performance criteria (Inequalities 9, 10, and 11) are met. Subsequently, the resulting performance vector:

$$\mathbf{x} = [x_1 \; x_2 \; x_3]^T$$

is used to compute two objective functions:

$$\|\mathbf{x}\|_1 = \sum_{i=1}^{3} x_i$$

$$\|\mathbf{x}\|_2 = \left[\sum_{i=1}^{3} x_i^2\right]^{\frac{1}{2}}$$

The performance vector and objective functions are returned to the optimization program by the post-processor to complete the design evaluation procedure.

3.9 Summary

This chapter presents the first formal statement of a lateral transverse fuel injection array design problem. Four design variables are used to propose possible designs: the fuel injection angle (δ_j), non-dimensional injector spacing (w/d_j^*), fuel jet total pressure (P_{T_j}), and fuel jet total temperature (T_{T_j}). Design performance is based on the penetration of the jet into the crossflow, the expansion of the fuel plume, and the decay of average fuel concentration in the jet. The problem is constrained by physical and manufacturing limitations on the design variables, and by the governing differential equations used in design evaluation to predict flow behavior. Finally, a design evaluation method is developed to facilitate optimization of the fuel injection array.

Chapter 4 - Optimization

4.1 Overview

This chapter presents the first stage of a VCM approach to scramjet fuel injection array design. Two optimization methods, Sequential Quadratic Programming and a Genetic Algorithm, are used in conjunction with *JETPEN* to seek an optimal design. As an initial step, a parametric analysis is conducted to explore the feasible design region. The information gained in this preliminary analysis is used to develop intelligent initial designs for the Sequential Quadratic Programming algorithm. The chapter concludes with a discussion of optimization algorithm performance and recommendations for future research.

4.2 Parametric Analysis

A parametric analysis of the scramjet fuel injection array problem is made possible by the simplicity and relative speed of design evaluation using the *JETPEN* software. Design performance is evaluated over a wide range of potential operating conditions to observe the behavior of, and interactions between, the design variables. In addition, parametric projections of the design space provide a sense of its topography, which is crucial to the selection, application, and evaluation of optimization algorithms.

There are six possible parametric combinations of the four design variables δ_j, w/d_j^*, P_{T_j}, and T_{T_j}. For each combination, two design variables are held constant while two are varied over a specified range. The constant values and ranges of variation for each design variable (**z**) are shown

Table 3. Parametric Ranges

z	Constant	Minimum	Maximum	Increment	Units
δ_j	30.0	15.0	60.0	3.0	deg
w/d_j^*	8.5	4.5	10.0	0.5	
P_{T_j}	200.0	100.0	640.0	30.0	psia
T_{T_j}	900.0	850.0	1510.0	30.0	^oR

in Table 3.

The responses for each performance measure and for the norms $\|\mathbf{x}\|_1$ and $\|\mathbf{x}\|_2$ are evaluated over the appropriate range for each parametric combination. Figures 11, 12, and 13 present surface plots of the variation of P_{T_j} and T_{T_j}, with δ_j and w/d_j^* held constant at 30^o and 8.5, respectively. Several trends are illustrated. First, the axial distance to centerline penetration (x_1) is minimized by operating at the minimum T_{T_j}. Increasing the injectant total temperature to a maximum of 1500^oR moves centerline penetration approximately one and one-half combustor heights ($1.5h$) downstream. Plume expansion (x_2) and fuel concentration decay (x_3) also occur more rapidly at lower T_{T_j}, though the dependence is somewhat weaker.

Second, there is an optimal P_{T_j} with respect to x_1 at approximately $130\,psia$. However, x_2 and x_3 are minimized at much larger values of P_{T_j}, and are extremely sensitive to pressure reductions. Consequently, decreasing P_{T_j} from 640 to 130 $psia$ moves x_1 approximately $0.5h$ upstream, but also moves x_2 and x_3 more than $5.0h$ downstream. This indicates that P_{T_j} must remain relatively high, and the corresponding slight reduction in penetration must be accepted in order to prevent major degradation of plume expansion and fuel concentration decay.

Further insights are gained from Figures 14, 15, and 16, in which δ_j and w/d_j^* are varied while P_{T_j} and T_{T_j} are held constant at 200 $psia$ and 900^oR, respectively. In particular, a reduction of more than $1.0h$ can be gained in both x_1 and x_3 by injecting at a relatively low angle. Extreme low angles, however, do not appear profitable as the benefits of decreasing δ_j much below 30^o are not significant. In addition, optimal w/d_j^* involves a trade-off between x_1 and x_3. Widely-spaced jets appear to result in more rapid penetration, while closely-spaced jets facilitate improved mixing.

Both sets of plots clearly indicate that the design space contains multiple local minima. A descent-based optimization method, such as Sequential Quadratic Programming (SQP), will generally converge to the local minimum closest to the initial design. Thus, to locate a global optimum,

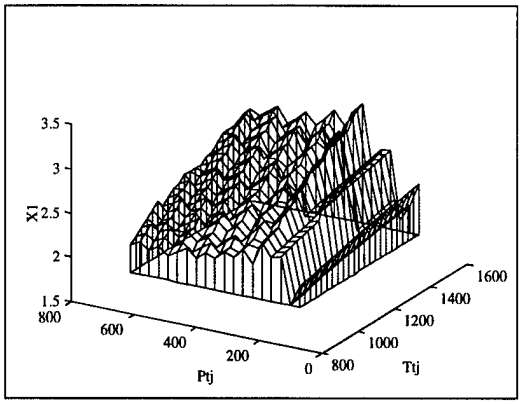

Figure 11. x_1 *vs.* Total Pressure and Total Temperature

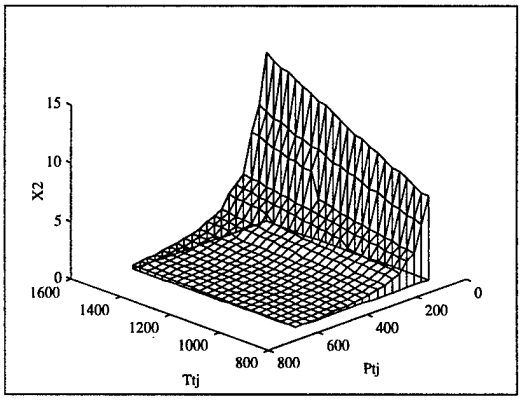

Figure 12. x_2 *vs.* Total Pressure and Total Temperature

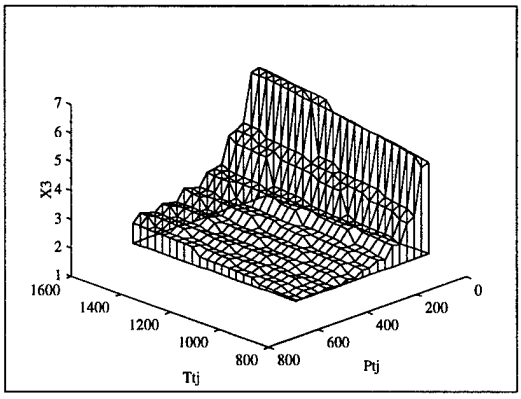

Figure 13. x_3 *vs.* Total Pressure and Total Temperature

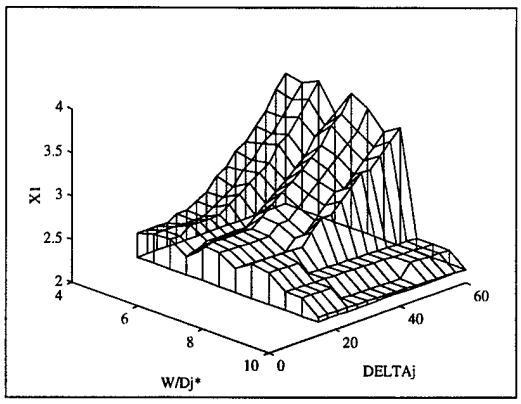

Figure 14. x_1 *vs.* Angle and Spacing

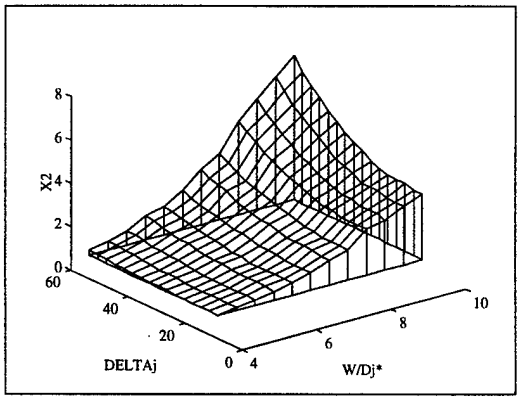

Figure 15. x_2 *vs.* Angle and Spacing

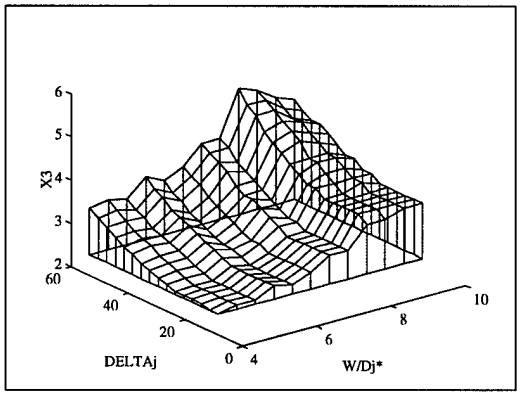

Figure 16. x_3 *vs.* Angle and Spacing

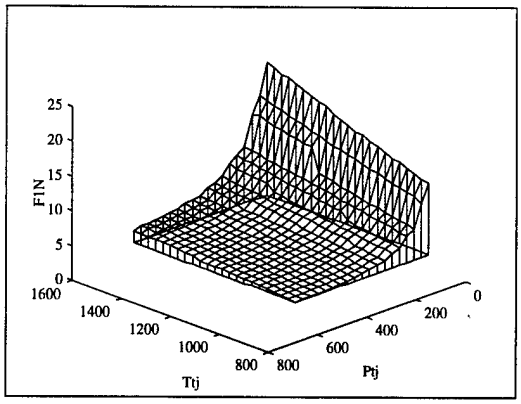

Figure 17. $\|\mathbf{x}\|_1$ *vs.* Total Pressure and Total Temperature

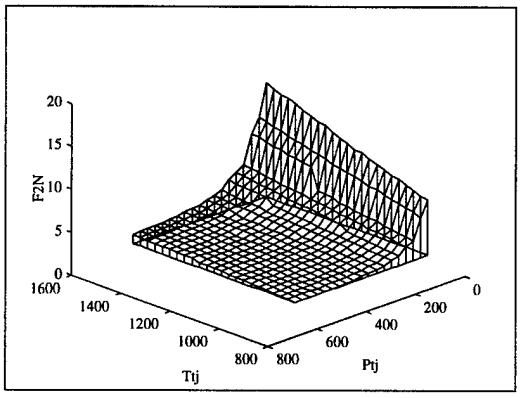

Figure 18. $\|\mathbf{x}\|_2$ *vs.* Total Pressure and Total Temperature

the SQP algorithm must begin with a design in the neighborhood of the global minimum. A rough estimate of the globally optimal neighborhood, developed from the parametric results, is provided in Table 4. This estimate is used in the following section to provide an initial design for the SQP

Table 4. Global Optimum Neighborhood

z	Region
δ_j	$\lessapprox 30^o$
$\frac{w}{d_i^*}$	$\lessapprox 9.0$
P_{T_j}	$\gtrapprox 250\ psia$
T_{T_j}	$\approx 850\ ^oR$

algorithm.

The plots of the performance vector norms are shown for P_{T_j} and T_{T_j} variation in Figures 17 and 18. These norm surfaces contain far fewer local optima than those of the individual performance criteria. Consequently, a choice of either $\|\mathbf{x}\|_1$ or $\|\mathbf{x}\|_2$ should outperform any single criterion as an objective function for this problem.

4.3 Sequential Quadratic Programming

Sequential Quadratic Programming (SQP) is a popular optimization method that has been used extensively in structural design [14] . While it is robust and efficient–particularly for large-scale problems–SQP is strictly a descent-based, local search method. Given a random starting design, the SQP algorithm will converge to the nearest local minimum. Because the preceding parametric analysis suggests the presence of multiple local minima, the success of SQP hinges on the selection of an initial design in the neighborhood of the global optimum.

One method of improving the chance of success is to employ SQP from multiple starting locations. This method usually requires a large number of starting designs to ensure sufficient coverage of the design space. *A priori* knowledge gained through the parametric analysis can, however, be used to significantly reduce the required number of initial designs.

4.3.1 Initial Designs

It is clear from Figures 11 through 16 and Table 4 that appropriate initial values for injection angle and jet total temperature are $\delta_j = 30^o$ and $T_{T_j} = 850^o R$, respectively. Appropriate values for jet spacing and total pressure are not as obvious. The parametric results suggest that high injection pressures such as $P_{T_j} = 600\, psia$ will most likely produce the best designs. However, there is some indication that a lower total pressure combined with a relatively close jet spacing may also yield a good design. These observations are used to select two initial designs for the SQP algorithm, which are listed in Table 5.

Table 5. SQP Initial Designs

Design	δ_j $(^o)$	$\mathbf{w/d_j^*}$	$\mathbf{P}_{T_j}$ $(psia)$	$\mathbf{T}_{T_j}$ (^oR)
1	30.0	5.75	300.0	850.0
2	30.0	8.50	600.0	850.0

4.3.2 Results

The SQP algorithm is executed 12 times: once with each of the six objective functions from both initial designs. The sequence $f = (x_3, x_1, x_2)$ is selected for the pareto objective function to ensure the most sensitive measures are optimized first. This ensures that concentration decay is not sacrificed for penetration, a situation revealed during the parametric analysis to produce sub-optimal results. The performance measures are used to compare the optimal designs obtained with the different objective functions. The decay of fuel concentration (x_3) provides the most direct indication of the point where ignition is possible, and is therefore considered the most important indicator of a good design. The remaining measures, however, are also important in assessing the overall progress of fuel-air mixing. Thus, superior designs are those with the smallest value of x_3, provided that the values x_1 and x_2 are also comparably small.

Optimization results from the first initial design are listed in Table 6. The left-hand column (**Obj F**) indicates the form of the objective function used, and each row is the resulting optimal design. The right-hand column (#**F**) is the number of function evaluations required to converge to the optimal design. As expected, objective functions that include all of the performance measures,

Table 6. SQP Initial Design 1 Results

Obj F	δ_j	$\mathbf{w/d}_j^*$	$\mathbf{P}_{T_j}$	$\mathbf{T}_{T_j}$	$\mathbf{x}_1$	$\mathbf{x}_2$	$\mathbf{x}_3$	#**F**
$\mathbf{x}_1$	30.594	5.716	321.40	852.13	2.274	0.404	2.114	199
$\mathbf{x}_2$	30.850	5.738	326.41	850.03	2.308	0.401	2.096	145
$\mathbf{x}_3$	30.034	5.750	306.36	850.01	2.326	0.412	1.998	148
$\|\mathbf{x}\|_1$	30.028	8.540	631.94	850.00	**2.207**	**0.365**	1.967	42
$\|\mathbf{x}\|_2$	30.071	5.757	326.19	850.08	2.256	0.402	2.045	153
Pareto	30.127	7.993	531.40	850.00	2.270	0.392	**1.964**	360

namely $\|\mathbf{x}\|_1$, $\|\mathbf{x}\|_2$,and the pareto approach, generally perform better than those based solely on individual criteria. The optimal design is produced by using $\|\mathbf{x}\|_1$as the objective function. The penetration and plume expansion distances are the shortest, and the fuel concentration decay is not significantly different than that achieved by the pareto approach. Furthermore, the pareto approach requires significantly more function evaluations (360) than the $\|\mathbf{x}\|_1$ objective function (42).

Interestingly, the $\|\mathbf{x}\|_1$ surface appears not to have a local optimum near $P_{T_j} = 300\ psia$, as exhibited by the other objective functions. Instead, an optimal design is located near $P_{T_j} \approx 632$ *psia*. While the higher pressure design is indeed superior, the performance increase is only slight. A comparison of the $\|\mathbf{x}\|_1$ and $\|\mathbf{x}\|_2$ designs indicates that doubling the injection pressure yields only a 4% improvement in fuel concentration decay.

The results from the second initial design are shown in Table 7. In this case, the best designs are produced by x_3 and the pareto approach. These objective functions do not, however, exhibit the best performance under general conditions. The parametric analysis clearly shows that exclusive focus on one performance measure can result in significant degradation of the others, indicating that

a choice of x_3 is not preferred. Furthermore, the x_3 surface contains far more local minima than the $\|\mathbf{x}\|_1$ and $\|\mathbf{x}\|_2$ surfaces, and thus is more likely to result in convergence to a sub-optimal result from a random starting location. The pareto approach is also not acceptable as it consistently requires a

Table 7. SQP Initial Design 2 Results

Obj F	δ_j	w/d_j^*	P_{T_j}	T_{T_j}	x_1	x_2	x_3	#F
x_1	30.000	8.500	600.003	850.000	2.263	0.414	1.935	11
x_2	33.962	8.042	618.718	853.682	2.346	0.347	2.038	100
x_3	30.000	8.591	615.111	850.000	2.236	0.410	**1.912**	42
$\|\mathbf{x}\|_1$	30.000	8.488	650.000	850.000	2.289	**0.343**	1.915	21
$\|\mathbf{x}\|_2$	30.032	7.854	607.960	850.000	**2.211**	0.352	1.979	44
Pareto	30.000	8.591	615.121	850.000	2.236	0.410	**1.912**	109

relatively large number of function evaluations and is thus unsuitable for use with more complex analysis methods. Thus, $\|\mathbf{x}\|_1$ is the preferred objective function for use with the SQP algorithm.

The results obtained from the second initial design are superior to those obtained from the first initial design. This confirms that the first initial design is in the neighborhood of a local minimum. Although it cannot be proven, the second initial design may be near the global minimum. Two observations support this assertion. First, the initial design was selected based on the parametric analysis results, and thus is suspected to be near-optimal. Second, $\|\mathbf{x}\|_1$ converged to virtually the same optimum from the two significantly different initial designs.

4.4 Genetic Algorithm

The parametric analysis provides a wealth of information regarding the design space of this problem. In fact, a feel for the topography is crucial to the success of the SQP algorithm. Parametric information, however, is available only at a high computational price: 1805 function evaluations were required to produce surface plots for the six parametric combinations. This was feasible using *JETPEN* for design evaluation, but would be nearly impossible with more elaborate analysis

methods such as CFD. Moreover, future studies will require an optimization method that does not rely on extensive parametric analysis to provide an initial design.

In this regard, genetic algorithms (GAs) represent a viable alternative to SQP. Since GAs do not rely on gradient information to improve the objective function, they are capable of avoiding local optima and thus succeeding where an SQP algorithm might fail. This section presents the application of a GA to the scramjet fuel injection array design problem.

4.4.1 Fitness Function

GAs converge to optima using a "survival of the fittest" strategy, and thus are naturally designed to maximize the performance, or *fitness*, of a system. To optimize the scramjet fuel injection array with a GA, the objective function is replaced with the following fitness function:

$$\text{maximize } F = F_{\max} - f(\mathbf{x})$$

where $F_{\max}$ is a constant selected to maintain a non-negative fitness function. $F_{\max} = 10.0$ is larger than the largest possible value of $f(\mathbf{x})$, and is thus a suitable choice for this problem. The performance measure norms $\|\mathbf{x}\|_1$ and $\|\mathbf{x}\|_2$ are used for $f(\mathbf{x})$ in the GA fitness function.

4.4.2 Constraints

GAs typically handle constraints by assigning a penalty to the fitness function if the proposed design violates a constraint. The proposal and evaluation of infeasible designs is not prevented by this method, and in fact may be encouraged by the GA during diversification of the search (mutation). This approach proved incompatible with *JETPEN* design evaluation, as extreme violations of the injector constraint, $3 \leq N \leq 10$, caused the software to abort.

As an alternative, N is calculated prior to design evaluation. If the proposed design violates the injector constraint, the evaluation routines are bypassed and the design is automatically assigned

a fitness value $F = 0$. Equation 22 (Appendix B), is rearranged and used to compute N:

$$N = \kappa \frac{P_{T_j}}{\left(\frac{w}{d_j^*}\right)^2 \sqrt{T_{T_j}}}$$

where

$$\kappa = \frac{\pi c_j^* l_f}{2 f A_r \dot{m}_{tot}}.$$

Since N is computed prior to design evaluation, an estimate of the ratio of specific heats ($\gamma_j = 1.113$) is used to calculate the jet discharge coefficient (c_j^*). The true value of γ_j varies from approximately 1.1 to 1.4 over the range of P_{T_j} and T_{T_j}, and thus some accuracy is sacrificed in the calculation of N. The injector constraint is relaxed to $2 \leq N \leq 11$ to allow for error in the estimate without eliminating potentially feasible designs.

4.4.3 Tuning Parameters

The GA used in this study [41] provides several options to improve algorithm performance. First, and perhaps most importantly, the user must specify the number of solutions to be maintained by the algorithm. Large populations are often used to maintain diversity and prevent the algorithm from converging prematurely to a sub-optimal result [22]. Population sizes ranging from 30 to 200 individuals are typical for this implementation, commonly known as a Simple Genetic Algorithm (SGA).

The primary drawback to SGAs is that large populations require a large number of design evaluations. As a result, modifications to the SGA have been proposed to reduce the required population size. Krishnakumar [28] reports impressive results with much smaller populations using a micro-Genetic Algorithm (μGA). The μGA maintains only 5 individuals, but monitors the population to detect premature convergence. Once the micro-population begins to converge, the most fit member is carried to the next generation and the remaining four members are replaced with new, randomly generated individuals. Thus, diversity is maintained in a small population without

the need for mutation. This method has reduced the number of required function evaluations by a factor of four in some cases [28] , [41] .

Both an SGA and a μGA are used to optimize the scramjet fuel injection array design. Population sizes of 32 and 5 are used for the SGA and μGA, respectively. Parent designs are identified by tournament selection and single-point crossover is used for reproduction. Only one child design per pair is produced in an effort to minimize the required number of function evaluations. Elitism is invoked in both cases to ensure the best known design is always passed to the next generation. Finally, both the SGA and μGA are initiated from several random populations to ensure the results are independent of the initial conditions.

4.4.4 Results

The GA optimization results are displayed in Table 8. The two left-most columns indicate the selected algorithm and fitness function; the rows contain the corresponding optimal solutions. In all

Table 8. GA Results

Algorithm	**Obj F**	δ_j	$\mathbf{w/d}_j^*$	$\mathbf{P}_{T_j}$	$\mathbf{T}_{T_j}$	$\mathbf{x}_1$	$\mathbf{x}_2$	$\mathbf{x}_3$	#F
SGA	$\|\mathbf{x}\|_1$	12.041	8.068	635.27	852.43	2.177	**0.284**	1.950	682
	$\|\mathbf{x}\|_2$	17.011	8.397	649.87	858.41	2.228	0.316	**1.891**	580
μGA	$\|\mathbf{x}\|_1$	11.739	7.797	580.14	855.49	2.237	0.333	1.960	368
	$\|\mathbf{x}\|_2$	15.116	7.803	603.41	850.06	**2.151**	0.325	1.956	159

cases, the algorithms converged to the same optimal design regardless of the random initial population. Superior designs are produced using $\|\mathbf{x}\|_2$ in the fitness function for both algorithms. From a practical standpoint, however, the designs are essentially equivalent. The optimal configurations are quite similar, and the fuel concentration decay performance of the best and worst designs differ by only $0.07h$, or roughly 4%. Thus both $\|\mathbf{x}\|_1$ and $\|\mathbf{x}\|_2$ are appropriate for use in a GA fitness function.

There is a dramatic difference in algorithm performance. Consider the two runs for which $\|\mathbf{x}\|_1$ is in the fitness function. The μGA requires 46% fewer function evaluations than the SGA to converge to an optimum. The reduction is nearly 73% for the runs containing $\|\mathbf{x}\|_2$ in the fitness function. Since the optimal designs are essentially equivalent, the μGA clearly outperforms the SGA for this problem.

4.5 Summary

The results for each optimization algorithm are summarized for comparison in Table 9. The

Table 9. Results Comparison

Algorithm	Obj F	δ_j	$\mathbf{w/d}_j^*$	$\mathbf{P}_{T_j}$	$\mathbf{T}_{T_j}$	$\mathbf{x}_1$	$\mathbf{x}_2$	$\mathbf{x}_3$	#F
SQP	$\|\mathbf{x}\|_1$	30.000	8.488	650.00	850.00	2.289	0.343	1.915	1826
SGA	$\|\mathbf{x}\|_2$	17.011	8.397	649.87	858.41	2.228	0.316	1.891	580
μGA	$\|\mathbf{x}\|_2$	15.116	7.803	603.41	850.06	2.151	0.325	1.956	159

performance characteristics of the three designs are remarkably similar; x_1, x_2, and x_3 differ at most by only $0.138h$, $0.027h$, and $0.065h$, respectively. The minimum axial distance required for fuel-air mixing is found to be approximately two combustor heights downstream of the injection point. In all cases, the optimal designs are characterized by a near-minimum jet total temperature ($850^o R$), a near-maximum jet total pressure (650 $psia$), and a maximum number of injectors (10). Furthermore, the SQP design, with an injection angle of 30^o, yields comparable performance to the lower-angle GA designs.

There is significant variation in the effort required by these algorithms to obtain an optimal solution. Although SQP appears to be most efficient, 1805 function evaluations are required to develop the initial design, and 21 additional evaluations are needed to locate the optimum. If, for example, the primary flow conditions are changed, a new parametric analysis is required to initiate the SQP algorithm. Thus, from a computational standpoint, SQP is prohibitively expensive and hence not a viable alternative for future research. The GAs are able to locate an optimal design

from random starting locations, and thus dramatically reduce computational cost. While both GA implementations represent a significant improvement over SQP, the μGA is two to four times more efficient than the SGA. This improvement will be crucial to integrating more sophisticated analysis methods with the design process. Moreover, the μGA is a particularly promising candidate for future research.

Chapter 5 - Response Surface Analysis

5.1 Overview

The objective of this chapter is to demonstrate a response surface methodology (RSM) approach to scramjet fuel injection array design. An appropriate experimental design is presented and used to construct a second-order meta-model of injector array performance. The meta-model is used to estimate an optimal design and predict the effects of design variable changes on overall system performance.

The most sophisticated design evaluation methods are typically used in this stage of VCM to maximize the quality of the final design. In this investigation, however, *JETPEN* is used for final-stage design evaluation since it is capable of providing reliable design assessments rapidly [7] ; time limitations precluded the use of CFD and/or experimental analysis methods in this study. This does not affect the RSM approach, but does limit the quality of the design solution to the accuracy of *JETPEN*. As such, the approach presented in this chapter is intended to serve as a basis for future research aimed at improving the design solution quality with CFD and/or experimental research methods.

5.2 Experimental Design

5.2.1 Design Region

The experimental design region is usually centered on the preliminary optimum design. In this case, however, both the SQP and GA designs (Table 9) are in close proximity to several constraint boundaries (Inequalities 4, 5, and 7). Since response data would be invalid in the infeasible regions, the design region is selected to include the SQP and GA optima, but encompass only feasible designs. For convenience in constructing the experimental design, the natural design variables

$(Z_i, i = 1..4)$ are transformed to coded variables (z_i) using the relation

$$z_i = \frac{Z_i - Z_{i,center}}{\frac{1}{2}(Z_{i,\max} - Z_{i,\min})}.$$

The transformation maps the design center to 0 and the design region limits to $[-1, +1]$. The design region is summarized in Table 10.

Table 10. Design Region

i	**Natural DV** (Z_i)	**Coded DV** (z_i)	**Minimum**	**Maximum**	**Units**
1	δ_j	A	10.0	30.0	deg
2	$\mathbf{w/d}_j^*$	B	7.5	9.5	
3	$\mathbf{P}_{T_j}$	C	550	650	psia
4	$\mathbf{T}_{T_j}$	D	850	950	^oR

5.2.2 Design Criteria

Two criteria are used to select an experimental design for scramjet fuel injection array investigation. First, both *JETPEN* and CFD analysis methods predict flowfield behavior by solving a deterministic set of governing differential equations. Since no random error is present in the solution algorithm, the experimental design is constructed to minimize the systematic bias. Second, this stage of VCM is intended to minimize the number of expensive design evaluations required to find an optimal solution. Thus, the number of experimental design points is held to a minimum.

To develop a minimum-bias design, the degree of the polynomial terms $(\mathbf{z}_1)$ in the meta-model

$$\widehat{y} = \mathbf{z}_1\widehat{\beta}_1$$

must be specified. The higher-order terms $(\mathbf{z}_2)$ to be protected against in the true model

$$E(y) = \mathbf{z}_1\beta_1 + \mathbf{z}_2\beta_2$$

must also be defined. Figures 17 and 18 provide strong evidence to suggest that a second-order polynomial is sufficient to approximate the $\|\mathbf{x}\|_1$ and $\|\mathbf{x}\|_2$ responses. Although higher-order effects are present, the predominant features of these surfaces are clearly second-order in nature. Thus, all possible first- and second-order combinations of the four design variables are included as model

terms in $\mathbf{z}_1$. To protect against third-order bias, the $\mathbf{z}_2$ model terms contain all third-order design variable combinations.

Given $\mathbf{z}_1$ and $\mathbf{z}_2$, a minimum-bias design is achieved with design moments set as follows (derived in Appendix C):

$$\begin{aligned} [ii] &\equiv \frac{1}{L}\sum_{u=1}^{L} z_{iu}^2 = \frac{1}{3} \\ [iiii] &\equiv \frac{1}{L}\sum_{u=1}^{L} z_{iu}^4 = \frac{1}{5} \\ [iijj] &\equiv \frac{1}{L}\sum_{u=1}^{L} z_{iu}^2 z_{ju}^2 = \frac{1}{9} \quad i \neq j \\ \text{all odd moments} &= 0 \\ i, j &= 1, 2, 3, 4 \end{aligned}$$

where i and j are design variable indices and L is the number of experimental levels. To ensure all odd moments are equal to zero, the design must be symmetric about its center. The number of experimental levels (L) must be specified to satisfy the remaining requirements. At least three levels are required to estimate the coefficients for a second-order model. For a symmetric three-level design $(-g, 0, g)$, the condition $[ii] = \frac{1}{3}$ yields

$$g = \sqrt{\frac{1}{2}} \approx 0.7071$$

and $[iiii] = \frac{1}{5}$ requires that

$$g = \left(\frac{3}{10}\right)^{\frac{1}{4}} \approx 0.7401.$$

Since no unique solution to these conditions exists, an absolute minimum-bias design cannot be constructed with only three levels of each design variable. Four design variable levels, set at $\pm f = \pm 0.7947$ and $\pm g = \pm 0.1876$, are necessary to satisfy all design moment requirements (see Appendix C).

A design constructed with four levels of each variable obviously requires more experiments than a three-level design. Because design evaluation is so expensive, it is more important to minimize the number of experiments than to achieve absolute minimum-bias in the experimental design. The minimum-bias criterion is therefore relaxed, and a near minimum-bias design, with $L = 3$, is developed and used for this problem (see Appendix C). The result is a central composite design for $n = 4$ design variables with the following 25 experimental design points:

- $2^n = 16$ factorial points at $\pm g = \pm\sqrt{\frac{1}{2}}$,
- $2n = 8$ axial points at $\pm a = 1$, and
- 1 center point.

5.3 Meta-Model

Performance data is collected with *JETPEN* at each of the experimental design points and least-squares regression is used to construct a surface to approximate the $\|\mathbf{x}\|_2$ response. The resulting meta-model is described by

$$\widehat{\|\mathbf{x}\|_2} = \mathbf{z}\widehat{\beta} \tag{12}$$

where the model terms ($\mathbf{z}$) and estimated coefficients ($\widehat{\beta}$) are summarized in Table 11.

Table 11. Response Surface Coefficients

Intercept	z_i	$\widehat{\beta}_i$	z_{ii}	$\widehat{\beta}_{ii}$	z_{ij}	$\widehat{\beta}_{ij}$
3.054682	A	0.012788	A^2	0.008614	AB	-0.004340
	B	0.017691	B^2	0.010649	AC	0.012024
	C	-0.016210	C^2	0.015703	AD	-0.005240
	D	0.096396	D^2	-0.001230	BC	-0.013510
					BD	0.001231
					CD	-0.001540

5.3.1 Model Adequacy

The statistical methods typically used to evaluate model adequacy and estimate effects are not applicable in this case due to the absence of random error. There are, however, two important indicators of model adequacy. First, the coefficient of determination (r^2) is a measure of the total

variation explained by the model. In this case, $r^2 = 0.990545$ indicating that the model accounts for over 99% of the variation. Second, the residuals, defined as the difference between actual and predicted responses ($\|\mathbf{x}\|_{2_i} - \widehat{\|\mathbf{x}\|_{2_i}}$), are used to identify model misspecification. Figure 19 is a plot of the residuals as a function of the predicted response ($\widehat{\|\mathbf{x}\|_2}$). The residuals appear to be randomly distributed about zero, which indicates the model is adequately specified.

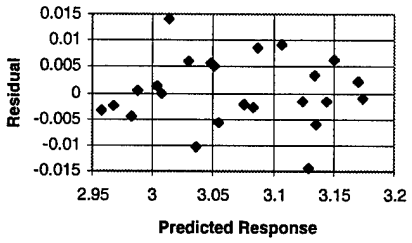

Figure 19. Residuals *vs.* Predicted Response

5.3.2 Optimization Results

An optimal solution to the second-order polynomial described by Equation 12 is shown in Table 12 (RSM). The fuel injection array designs from SQP and GA optimization are included for comparison. The RSM array design is quite similar to the SQP and GA designs, providing further evidence that the RSM meta-model is a good approximation to the true array performance within this design region. The similarity of these designs also indicates that the use of a near, rather than absolute, minimum-bias experimental design does not significantly affect the results. Most importantly, RSM yields a comparable fuel injection array design with only 25 experiments–just 16% of the design evaluations required by the most efficient optimization algorithm.

5.3.3 Sensitivity

The results in Table 12 suggest that design performance depends strongly on the jet total temperature, as $T_{T_j} \approx 850^o R$ in all four cases. Furthermore, the performance is relatively insensitive to injection angle changes between 10^o and 30^o. These assertions are tested by changing each design variable independently at equal coded-space increments $\left(0, \frac{1}{3}, \frac{2}{3}, 1\right)$ and evaluating the design performance ($\|\mathbf{x}\|_2$). The results, illustrated in Figure 20, confirm that design performance in this

Table 12. Response Surface Results

Algorithm	Obj F	δ_j	w/d_j^*	P_{T_j}	T_{T_j}	x_1	x_2	x_3	#F
SQP	$\|\mathbf{x}\|_1$	30.000	8.488	650.00	850.00	2.289	0.343	1.915	1826
SGA	$\|\mathbf{x}\|_2$	17.011	8.397	649.87	858.41	2.228	0.316	1.891	580
μGA	$\|\mathbf{x}\|_2$	15.116	7.803	603.41	850.06	2.151	0.325	1.956	159
RSM	$\|\mathbf{x}\|_2$	10.000	7.898	629.56	850.00	2.229	0.273	1.903	25

region is affected most by changes in T_{T_j}, and is unaffected by changes in δ_j. Even changes in T_{T_j}, however, reduce the performance by less than $0.07h$ over this range. Thus, there is considerable flexibility in the design variable settings in the region surrounding the optimal design.

A canonical analysis of the meta-model provides similar information in the absence of parametrics and conventional optimization results. The eigenvalues of the symmetric matrix:

$$B = \begin{bmatrix} \widehat{\beta}_{11} & \cdots & \widehat{\beta}_{14} \\ \vdots & \ddots & \vdots \\ \widehat{\beta}_{14} & \cdots & \widehat{\beta}_{44} \end{bmatrix}$$

characterize the nature of the response surface at the design center: larger eigenvalues imply greater sensitivity in the direction of the corresponding eigenvector. In this case, the eigenvalues of B are all extremely small:

$$\lambda = \begin{bmatrix} -0.00098 \\ -0.00518 \\ 0.00642 \\ 0.03300 \end{bmatrix}$$

indicating that the response surface is nearly flat. Thus, design performance is relatively constant over the design region. The relative magnitudes of the coefficients are indicators of performance

sensitivity to the individual factors. The jet total temperature coefficient ($\widehat{\beta}_4$) is roughly an order of magnitude larger than the coefficients of the other first-order terms. This reflects the strong relative influence of T_{T_j} in the design region. Finally, optimization of the meta-model provides the Lagrange multipliers -0.0105 and -0.1024 for the constraints on δ_j and T_{T_j}, respectively. The absolute and relative magnitudes of these multipliers confirm that the design region is relatively flat, and that a jet total temperature increase will degrade performance more than an increase in the injectant angle.

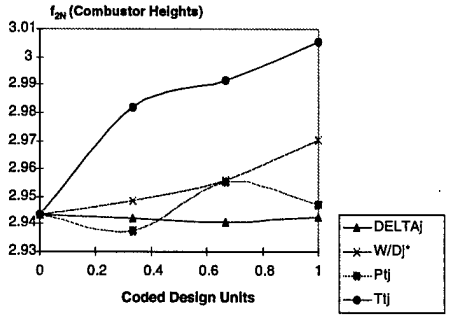

Figure 20. Performance Sensitivity

5.4 Summary

The RSM approach results in an adequate second-order meta-model of the true fuel injection array performance. The meta-model optimum is remarkably similar to the designs found with the SQP and GA algorithms. An axial distance of approximately two combustor heights is required to meet the three performance criteria, and the design is characterized by a minimum jet total temperature and a near-maximum jet total pressure. Furthermore, a canonical analysis reveals that the design variables can be altered within the design region limits without significantly affecting performance.

In contrast to the SQP and GA methods, RSM requires only 25 experiments to locate the optimal design. RSM is thus established as a feasible method for use in conjunction with CFD and experimental research. However, RSM accuracy is contingent on the use of SQP and GA results to select an appropriate experimental design region. The VCM approach is therefore necessary to obtain accurate results while capitalizing on the efficiency of RSM.

Chapter 6 - Conclusion

6.1 Summary

Fuel injection in a supersonic crossflow is still a challenging research problem, and thus little effort has been devoted to array design in the context of traditional optimization. This research presents the first formal statement of a lateral transverse fuel injection array design problem. Four design variables are used to propose possible designs: the fuel injection angle (δ_j), non-dimensional injector spacing (w/d_j^*), fuel jet total pressure (P_{T_j}), and fuel jet total temperature (T_{T_j}). Design performance is based on the penetration of the jet into the crossflow, the expansion of the fuel plume, and the decay of average fuel concentration in the jet. The problem is constrained by physical limitations on the design variables, and by the governing differential equations used in design evaluation to predict flow behavior.

Design evaluation is typically accomplished with computational fluid dynamics (CFD) methods and/or experimental research, both of which are extremely time-consuming and expensive. However, these methods are not suitable for use with conventional optimization methods, which often require thousands of evaluations to reach an optimal solution. This research presents a two-stage Variable-Complexity Modeling (VCM) approach designed to minimize the cost of optimizing the scramjet fuel injection array.

In the first stage, a simplified analysis method, *JETPEN*, is used to provide rapid, inexpensive design performance evaluations. An initial parametric analysis illuminates three important trends. First, array performance, and particularly penetration, is improved by minimizing the jet total temperature. Second, fuel concentration decay and plume expansion occur more rapidly, and penetration to the combustor centerline is delayed, at higher jet total pressures. The penetration delay is slight, however, and must be accepted in order to prevent major degradation of plume expansion and

fuel concentration decay. Finally, relatively low injection angles yield superior array performance, but gains realized for δ_j much below 30^o are not significant.

Two optimization methods, Sequential Quadratic Programming (SQP) and a Genetic Algorithm (GA), are used in the first stage to develop a preliminary optimal design. The minimum axial distance required for fuel-air mixing is found to be approximately two combustor heights downstream of the injection point. Both algorithms yield designs that are consistent with the parametric analysis results. In all cases, the optimal designs are characterized by a near-minimum jet total temperature (850^oR), a near-maximum jet total pressure (650 $psia$), and a maximum number of injectors (10). Furthermore, the SQP design, with an injection angle of 30^o, yields comparable performance to the lower-angle GA designs.

In the second stage, response surface methodology (RSM) is used to minimize the required number of expensive, complex analyses required to verify initial stage results and finalize the design. A near minimum-bias experimental design is developed and used to construct a second-order meta-model of fuel-injection array performance. The meta-model yields an optimal design similar to those found with the SQP and GA algorithms. In addition, the response surface illuminates a relatively flat region in the neighborhood of the optimal design. As design performance is relatively constant over this region, there is considerable flexibility in the design variable settings. Performance is found to be most sensitive to jet total temperature changes, and relatively unaffected by changes to the injection angle.

There is significant variation in the effort required by these algorithms to obtain an optimal solution. SQP success depends heavily on the initial design developed through parametric analysis. Thus, from a computational standpoint, SQP is prohibitively expensive. The GAs locate an optimal design from random starting locations, and thus dramatically reduce computational cost. A μGA is used to locate an optimum in 159 design evaluations, as compared to 1826 and 580 required by SQP

and an SGA, respectively. The RSM approach requires just 25 experiments to locate an optimal design, but relies on initial stage information to define the design region.

6.2 Recommendations

This investigation clearly establishes the potential of a Variable-Complexity Modeling approach to scramjet fuel injection array design. Continued research must begin with a verification of the results and an evaluation of *JETPEN* effectiveness. The response surface approach demonstrated in this investigation should be used in conjunction with both CFD and experimental research techniques to quantify the effects of total pressure losses on the optimal design. Recommendations for such an investigation are described below.

Preliminary Optimum Verification. An initial experiment should be conducted to verify the performance of the preliminary optimal design. The μGA design:

Obj F	δ_j	$\mathbf{w/d}_j^*$	$\mathbf{P}_{T_j}$	$\mathbf{T}_{T_j}$	$\mathbf{x}_1$	$\mathbf{x}_2$	$\mathbf{x}_3$	**N**	d_j^*
$\|\mathbf{x}\|_2$	15.116	7.803	603.41	850.06	2.151	0.325	1.956	10	0.0734"

should be verified, as the μGA will most likely be the algorithm of choice for future research.

Response Surface Analysis. Since CFD, like *JETPEN*, is a deterministic design evaluation procedure, the near minimum-bias experimental design derived in Appendix C should be used to construct a meta-model of injection array performance. A similar surface should be construct using experimental methods, but the introduction of measurement error will require the use of an alternate experimental design. For this effort, the CCD structure with factorial points at $\pm g = \pm 1$ and axial points at $\pm a = \sqrt{2}$ provides a more appropriate, variance-optimal design. The experimental investigation results should be used to validate and/or suggest modifications to the *JETPEN* and CFD software.

An important extension to this research is the investigation of different mission parameters and array configurations. The effects of the following parameters on the optimal design are of particular interest.

Primary Flow Conditions. The conditions at the combustor entrance significantly affect mixing and penetration performance. The μGA and *JETPEN* software should be used to investigate combinations of the primary flow Mach number, total pressure, and total temperature that are of current interest.

Fuels. Alternate fuel types may also affect design performance. To investigate the effects of different fuels, such as JP-7, additional polynomial approximations must be added to the preprocessing routine to calculate the ratio of specific heats from proposed fuel conditions.

Injection Array Configuration. The staged-array, or aero-ramp, configuration is one of the most promising developments in this field of research. To study an aero-ramp configuration, the design problem must be revised to include at least two additional design variables: the injection angle of the aero-ramps, and the spacing between the primary and aero-ramp fuel injectors. Currently, aero-ramp design evaluation is possible only with CFD and experimental research methods. A simplified analysis method, perhaps an extension to *JETPEN*, is needed to fully study aero-ramp configurations in an optimization context. In the interim, the response surface approach presented in this investigation can be readily applied to aero-ramp configurations.

APPENDIX A - Design Problem Parameters

The following tables contain the parameters used for this optimization study. All parameter values were specified by the High Speed Systems Development Branch, Propulsion Sciences and Advanced Concepts Division, Propulsion Directorate, Air Force Research Laboratory, Wright-Patterson AFB, OH (AFRL/PRSS).

A.1 Primary Flow Conditions

Parameter	Description	Value	Units
M_a	Mach Number	1.80	
P_{T_a}	Total Pressure	141.10	psia
T_{T_a}	Total Temperature	3140.00	^{o}R
γ_a	Ratio of Specific Heats	1.35	
c_{p_a}	Specific Heat	0.27	$\frac{BTU}{lb_m\ ^oR}$
w_a	Molecular Weight	28.37	

A.2 Combustion Parameters

Parameter	Description	Value
$Fuel$	Ethylene	
w_f	Fuel Molecular Weight	28.05400
f_{ST}	Stoichiometric Fuel/Air Ratio	0.06809
Φ	Equivalence Ratio	0.90000

A.3 Combustor Geometry

Parameter	Description	Value	Units
l	Combustor Width	7.000	in
l_f	Fueled Combustor Width	6.000	in
l_{nf}	Unfueld Combustor Width	1.000	in
h	Combustor Height	2.567	in

APPENDIX B - Fuel Injector Design Equations

This section presents the analysis method used by the fuel injector design subroutine to calculate the required injector diameter (d_j^*) and number of injectors (N).

B.1 Primary Flow Total Mass Flow Rate

The total mass flow rate of the primary flow is given by:

$$\dot{m}_{tot} = \varrho U A$$

Assuming the flow behaves as a perfect gas, this can be written:

$$\dot{m}_{tot} = \frac{P_a}{R_a T_a} M_a a_a A \tag{13}$$

where:

$$\begin{aligned} R_a &= \frac{R_u}{w_a} \\ a_a &= [\gamma_a R_a T_a]^{\frac{1}{2}} \\ A &= lh \end{aligned}$$

and l is the combustor width and h is the combustor height. The primary flow static conditions are calculated with the following isentropic relations:

$$T_a = \frac{T_{T_a}}{[1 + \frac{\gamma_a - 1}{2} M_a^2]} \tag{14}$$

$$P_a = \frac{P_{T_a}}{[1 + \frac{\gamma_a - 1}{2} M_a^2]^{\frac{\gamma_a}{\gamma_a - 1}}} \tag{15}$$

Thus, the total mass flow rate can be calculated using equation 13 with the specified primary flow conditions $M_a, P_{T_a}, T_{T_a}, \gamma_a, w_a$ and the combustor dimensions l, h.

B.2 Injector Diameter

Once the total mass flow rate is known, the proportion of air mass flow fueled by each injector is calculated. The area fueled by a single injector (A_i) is given by:

$$A_i = \frac{[A - A_{nf}]}{2N}$$

where A_{nf} is included in case of any non-fueled area in the combustor. The distinction between fueled and non-fueled area is included to account for cases in which manufacturing restrictions prevent the installation of injectors within a prescribed distance from the combustor sidewalls. If no such restriction exists, $A_{nf} = A$ and $A_i = (2N)^{-1}$. The factor of 2 is included in the denominator because N represents only half of the total injectors due to the symmetry assumption. It follows that the fractional mass flow rate for a single injector is:

$$\dot{m}_a = \frac{A_i}{A}\,\dot{m}_{tot} = \frac{1}{2N} A_r\,\dot{m}_{tot} \tag{16}$$

where:

$$A_r = 1 - \frac{A_{nf}}{A}$$

The required fuel mass flow rate for each injector is simply:

$$\dot{m}_f = f\,\dot{m}_a \tag{17}$$

where:

$$f = \Phi f_{ST}$$

Recall that the equivalence ratio (Φ) and stoichiometric fuel-air ration (f_{ST}) are specified parameters. Substituting equation 16 into equation 17 yields:

$$\dot{m}_f = \frac{1}{2N} f A_r\,\dot{m}_{tot} \tag{18}$$

The fuel mass flow rate may also be derived from continuity, yielding:

$$\dot{m}_f = \frac{P_{T_j} A_j^* c_j^*}{\sqrt{T_{T_j}}} \tag{19}$$

Equating 18 and 19 and solving for the jet area yields:

$$A_j^* = \frac{f A_r\,\dot{m}_{tot}\,\sqrt{T_{T_j}}}{2N P_{T_j} c_j^*}$$

This equation is then substituted into the geometric definition of the injector diameter:

$$d_j^* = \left[\frac{4A_j^*}{\pi}\right]^{\frac{1}{2}}$$

to yield an equation for the jet diameter based on the design variables, prescribed combustor size, primary flow conditions:

$$d_j^* = \left[\frac{4 f A_r \dot{m}_{tot} \sqrt{T_{T_j}}}{\pi 2 N P_{T_j} c_j^*} \right]^{\frac{1}{2}}$$

To simplify the ensuing presentation, let:

$$Q = \frac{4 f \dot{m}_{tot} \sqrt{T_{T_j}}}{\pi P_{T_j} c_j^*} \tag{20}$$

such that the jet diameter may be conveniently expressed as:

$$d_j^* = \left[\frac{1}{2N} A_r Q \right]^{\frac{1}{2}} \tag{21}$$

B.3 Number of Injectors

In general, the number of injectors (N) is given by:

$$N = \frac{l_f}{w}$$

where l_f is the width the combustor allowed to contain injectors and w is the distance between adjacent jets. Dividing the numerator and denominator by d_j^* and using equation 21 yields:

$$N = \frac{l_f}{\frac{w}{d_j^*} \left[\frac{1}{2N} A_r Q \right]^{\frac{1}{2}}}$$

Finally, solving this for the number of injectors yields:

$$N = \frac{2 l_f^2}{A_r Q \left(\frac{w}{d_j^*} \right)^2} \tag{22}$$

The number of injectors can now be calculated directly from the design variables and prescribed parameters using Equation 22. Subsequently, the injector diameter can be calculated with Equation 21.

APPENDIX C - Experimental Design

This appendix presents the development of the near minimum-bias design used to construct the scramjet fuel injection array performance meta-model.

C.1 Definitions

The design region (R) is defined to be cuboidal in coded space, such that:

$$z_i \in [-1, 1], i = 1..4$$

The meta-model:

$$\widehat{y} = \mathbf{z}_1 \widehat{\beta}_1$$

is assumed to be a second-order approximation to the true model:

$$E(y) = \mathbf{z}_1 \beta_1 + \mathbf{z}_2 \beta_2$$

such that the design matrix is defined as:

$$Z_1 = \begin{bmatrix} 1 & z_{1_1} & \cdots & z_{4_1} & z_1 z_{2_1} & \cdots & z_3 z_{4_1} & z_{1_1}^2 & \cdots & z_{4_1}^2 \\ \vdots & \vdots & & \vdots & \vdots & & \vdots & \vdots & & \vdots \\ 1 & z_{1_L} & \cdots & z_{4_L} & z_1 z_{2_L} & \cdots & z_3 z_{4_L} & z_{1_L}^2 & \cdots & z_{4_L}^2 \end{bmatrix}$$

where L is the number of experimental observations. The design is constructed to protect against third-order bias given by the matrix:

$$Z_2 = \begin{bmatrix} z_1 z_2 z_{3_1} & \cdots & z_2 z_3 z_{4_1} & z_{1_1}^3 & \cdots & z_{4_1}^3 \\ \vdots & & \vdots & \vdots & & \vdots \\ z_1 z_2 z_{3_L} & \cdots & z_2 z_3 z_{4_L} & z_{1_L}^3 & \cdots & z_{4_L}^3 \end{bmatrix}$$

C.2 Derivation

The average squared bias (ASB) of a design is given by:

$$ASB = \frac{\sqrt{L}}{\sigma} \beta_2^T \left[\left(\mu_{22} - \mu_{12}^T \mu_{11}^{-1} \mu_{12} \right) + \left(M_{11}^{-1} M_{12} - \mu_{11}^{-1} \mu_{12} \right)^T \mu_{11} \left(M_{11}^{-1} M_{12} - \mu_{11}^{-1} \mu_{12} \right) \right] \frac{\sqrt{L}}{\sigma} \beta_2^T$$

Sufficient conditions for minimizing the ASB over the region of interest are [29] :

$$M_{11} = \mu_{11} \text{ and } M_{12} = \mu_{12}$$

such that the quantity (B):

$$B \equiv \left(M_{11}^{-1} M_{12} - \mu_{11}^{-1} \mu_{12} \right)^T \mu_{11} \left(M_{11}^{-1} M_{12} - \mu_{11}^{-1} \mu_{12} \right)$$

is equal to zero for a minimum-bias design. Thus, development of the experimental design consists of setting the design moment matrices:

$$M_{11} = \frac{Z_1^T Z_1}{L} \text{ and } M_{12} = \frac{Z_1^T Z_2}{L}$$

equal to the region moment matrices:

$$\mu_{11} = K \int_R \mathbf{z}_1 \mathbf{z}_1^T d\mathbf{z} \text{ and } \mu_{12} = K \int_R \mathbf{z}_1 \mathbf{z}_2^T d\mathbf{z}$$

K is the inverse of the region volume, such that:

$$\begin{aligned} K &= \left[\int \int \int \int_{-1}^{1} dz_1 dz_2 dz_3 dz_4 \right]^{-1} \\ &= \frac{1}{16} \end{aligned}$$

Thus,

$$\mu_{11} = \frac{1}{16} \int_R \mathbf{z}_1 \mathbf{z}_1^T d\mathbf{z} \text{ and } \mu_{12} = \frac{1}{16} \int_R \mathbf{z}_1 \mathbf{z}_2^T d\mathbf{z}$$

The integration over R cancels out all terms in the region moment matrices that contain a design variable raised to an odd power, since:

$$\int_{-1}^{1} z_i^n dz_i = 0, \forall \text{ odd } n.$$

Similarly, all pure quadratic terms integrate to $\frac{1}{3}$, pure fourth-order terms integrate to $\frac{1}{5}$, and the interaction of pure quadratic terms integrates to $\frac{1}{9}$.

Since M_{11} and M_{12} are matrices containing the design moments, the sufficient conditions yield:

$$\begin{aligned}
[ii] &\equiv \frac{1}{L}\sum_{u=1}^{L} z_{iu}^2 = \frac{1}{3} \\
[iiii] &\equiv \frac{1}{L}\sum_{u=1}^{L} z_{iu}^4 = \frac{1}{5} \\
[iijj] &\equiv \frac{1}{L}\sum_{u=1}^{L} z_{iu}^2 z_{ju}^2 = \frac{1}{9} \quad i \neq j \\
\textit{all odd moments} &= 0 \\
i,j &= 1..4
\end{aligned}$$

For a symmetric three-level design $(-g, 0, g)$, the condition $[ii] = \frac{1}{3}$ yields:

$$\begin{aligned}
\frac{1}{3}\left[(-g)^2 + 0^2 + g^2\right] &= \frac{1}{3} \\
g &= \sqrt{\frac{1}{2}} \approx 0.7071
\end{aligned}$$

and $[iiii] = \frac{1}{5}$ requires that:

$$\begin{aligned}
\frac{1}{3}\left[(-g)^4 + 0^4 + g^4\right] &= \frac{1}{5} \\
g &= \left(\frac{3}{10}\right)^{\frac{1}{4}} \approx 0.7401
\end{aligned}$$

yielding no unique solution. A unique, minimum-bias solution does exist for a four-level design:

$$\begin{aligned}
\pm f &= \pm 0.7947 \\
\pm g &= \pm 0.1876
\end{aligned}$$

However, a three-level design is preferred to minimize the required number of experiments. The minimum-bias criterion is relaxed by setting $g = \sqrt{\frac{1}{2}}$, thereby violating the condition $[iiii] = \frac{1}{5}$. This compromise yields $[iiii] = \frac{1}{6}$ and results in:

$$\begin{aligned}
B &= \left(M_{11}^{-1}M_{12} - \mu_{11}^{-1}\mu_{12}\right)^T \mu_{11} \left(M_{11}^{-1}M_{12} - \mu_{11}^{-1}\mu_{12}\right) \\
&= \frac{1}{300} \approx 0.0033
\end{aligned}$$

Since $B \neq 0$, the ASB is not minimized and this design is described as near minimum-bias.

C.3 Structure

The familiar Central Composite Design structure is used for experimentation in this investigation. Factorial and axial points are located at $\pm g = \sqrt{\frac{1}{2}}$ and $\pm a = 1$, respectively. The full experimental design is shown below.

$$\begin{bmatrix}
+g & +g & +g & +g \\
-g & +g & +g & +g \\
+g & -g & +g & +g \\
-g & -g & +g & +g \\
+g & +g & -g & +g \\
-g & +g & -g & +g \\
+g & -g & -g & +g \\
-g & -g & -g & +g \\
+g & +g & +g & -g \\
-g & +g & +g & -g \\
+g & -g & +g & -g \\
-g & -g & +g & -g \\
+g & +g & -g & -g \\
-g & +g & -g & -g \\
+g & -g & -g & -g \\
-g & -g & -g & -g \\
+a & 0 & 0 & 0 \\
-a & 0 & 0 & 0 \\
0 & +a & 0 & 0 \\
0 & -a & 0 & 0 \\
0 & 0 & +a & 0 \\
0 & 0 & -a & 0 \\
0 & 0 & 0 & +a \\
0 & 0 & 0 & -a \\
0 & 0 & 0 & 0
\end{bmatrix}$$

BIBLIOGRAPHY

[1] W. H. Heiser and D. T. Pratt. *Hypersonic Airbreathing Propulsion.* American Institute of Aeronautics and Astronautics, Inc., Washington DC, 1994.

[2] McClinton C.R. Rausch, V.L. and J.W. Hicks. Scramjets breathe new life into hypersonics. *Aerospace America*, 35(7):40–46, 1997.

[3] Schetz J.A. Thomas, R.H. and F.S. Billig. Gaseous injection in high speed flow. In *Ninth International Symposium on Air Breathing Engines*, Athens, Greece, September 3-8 1989.

[4] Nejad A.S. Chen T.H. Gruber, M.R. and J.C. Dutton. Compressibility effects in supersonic transverse injection flowfields. *Physics of Fluids*, 9(5):1448–1461, May 1997.

[5] Thomas R.H. Mays, R.B. and J.A. Schetz. Low angle injection into a supersonic flow. In *25th AIAA/ASME/SAE/ASEE Joint Propulsion Conference*, Monterey, CA, July 10-12 1989. AIAA-89-2461.

[6] Bowersox R. Wilson, M. and D. Glawe. The role of downstream ramps on penetration and mixing enhancement for supersonic injection flows. In *33rd AIAA/ASME/SAE/ASEE Joint Propulsion Conference and Exhibit*, Seattle, WA, July 7-9 1997.

[7] F.S. Billig and J.A. Schetz. Analysis of penetration and mixing of gas jets in supersonic cross flow. In *AIAA Fourth International Aerospace Planes Conference*, Orlando, FL, December 1-4 1992. AIAA-92-5061.

[8] R.C. Rodgers. Mixing of hydrogen injected from multiple injectors normal to a supersonic airstream. Technical Report NASA TN D-6476, NASA Langley Research Center, Hampton, VA, September 1971.

[9] C.R. McClinton. The effect of injection angle on the interaction between sonic secondary jets and a supersonic free stream. Technical Report NASA TN D-6669, NASA Langley Research Center, Hampton, VA, February 1972.

[10] J.A. Schetz and F.S. Billig. Penetration of gaseous jets injected into a supersonic stream. *Journal of Spacecraft and Rockets*, 3(11):1658–1665, November 1966.

[11] McDaniel J.C. Hollo, S.D. and R.J. Hartfield. Quantitative investigation of compressible mixing: Staged transverse injection into mach 2 flow. *AIAA Journal*, 32(3):528–534, March 1994.

[12] J.S. Arora. *Introduction to Optimum Design.* McGraw-Hill, Inc., New York, 1989.

[13] S.S. Rao. *Engineering Optimization: Theory and Practice.* John Wiley and Sons, Inc., New York, 1996.

[14] Arora J.S. Tseng C.H. Lim O.K. Thanedar, P.B. and G.J. Park. Performance of some sqp algorithms on structural design problems. *International Journal for Numerical Methods In Engineering*, 23:2187–2203, 1986.

[15] A.D. Belegundu and J.S. Arora. A recursive quadratic programming method with active set strategy for optimal design. *International Journal For Numerical Methods In Engineering*, 20:803–816, 1984.

[16] M.A. Abramson. Application of sequential quadratic programming to large-scale structural

design problems. Master's thesis, Air Force Institute of Technology, Wright-Patterson AFB, OH, March 1994.

[17] A.H.G. Rhinnooy Kan and G.T. Timmer. A stochastic approach to global optimization. In Byrd R.H. Boggs, P.T. and R.B. Schnabel, editors, *Numerical Optimization 1984*, pages 245–262, Philadelphia, PA, 1985. Society for Industrial and Applied Mathematics.

[18] A.V. Levy and S. Gomez. The tunneling method applied to global optimization. In Byrd R.H. Boggs, P.T. and R.B. Schnabel, editors, *Numerical Optimization 1984*, pages 213–244, Philadelphia, PA, 1985. Society for Industrial and Applied Mathematics.

[19] M. Pirlot. General local search methods. *European Journal of Operational Research*, 92:493–511, 1996.

[20] Marconi F. Ogot M. Pelz R. Aly, S. and M. Siclari. Stochastic optimization applied to cfd shape design. In *12th AIAA Computational Fluid Dynamics Conference*, San Diego, CA, June 19-22 1995. AIAA-95-1647-CP.

[21] Aly S. Pelz R. Marconi F. Ogot, M. and M. Siclari. Stochastic versus gradient-based optimizers for cfd shape design. In *34th Aerospace Sciences Meeting and Exhibit*, Reno, NV, January 15-18 1996. AIAA-96-0332.

[22] D.E. Goldberg. *Genetic Algorithms in Search, Optimization, and Machine Learning*. Addison-Wesley, Reading, MA, 1989.

[23] P. Hajela. Genetic search – an approach to the nonconvex optimization problem. In *32nd AIAA/ASME/ASCE/AHS/ASC Structures, Structural Dynamics, and Materials Conference*, Baltimore, MD, April 8-10 1991.

[24] K. Deb. Optimal design of a class of welded structures via genetic algorithms. In *31st AIAA/ASME/ASCE/AHS/ASC Structures, Structural Dynamics, and Materials Conference*, Long Beach, CA, April 2-4 1990.

[25] S. Obayashi and T. Tsukahara. Comparison of optimization algorithms for aerodynamic shape design. In *14th AIAA Applied Aerodyanmics Conference*, New Orleans, LA, June 17-20 1996.

[26] M.B. Anderson. The potential of genetic algorithms for subsonic wing design. In *1st AIAA Aircraft Engineering, Technology, and Operations Congress*, Los Angeles, CA, September 19-21 1995.

[27] N.F. Foster and G.S. Dulikravich. Three-dimensional aerodynamic shape optimization using genetic and gradient search algorithms. *Journal of Spacecraft and Rockets*, 34(1):36–42, January-February 1997.

[28] K. Krishnakumar. Micro-genetic algorithms for stationary and non-stationary function optimization. In *SPIE: Intelligent Control and Adaptive Systems, Vol. 1196*, Philadelphia, PA, 1989.

[29] R.H. Myers and D.C. Montgomery. *Response Surface Methodology: Process and Product Optimization Using Designed Experiments*. John Wiley and Sons, Inc., New York, 1995.

[30] M.J. Box and N.R. Draper. On-minimum point second-order designs. *Technometrics*, 16(4), November 1974.

[31] Lepsch R.A. Engelund W. Unal, R. and D.O. Stanley. Approximation model building and multidisciplinary design optimization using response surface methods. In *6th AIAA/NASA/ISSMO Symposium on Multidisciplinary Analysis and Optimization*, Bellevue, WA, September 4-6 1996. AIAA-96-4044-CP.

[32] Allen J.K. Schrage D.P. Chen, W. and F. Mistree. Statistical experimentation for affordable concurrent design. In *6th AIAA/NASA/ISSMO Symposium on Multidisciplinary Analysis and Optimization*, Bellevue, WA, September 4-6 1996. AIAA-96-4085.

[33] Stander N. Roux, W.J. and R.T. Haftka. Response surface approximations for structural optimization. In *6th AIAA/NASA/ISSMO Symposium on Multidisciplinary Analysis and Optimization*, Bellevue, WA, September 4-6 1996. AIAA-96-4042.

[34] G. Venter and R.T. Haftka. Minimum-bias based experimental design for constructing response surfaces in structural optimization. In *AIAA/ASME/ASCE/AHS/ASC 38th Structures, Structural Dynamics, and Materials Conference and Exhibit*, Kissimmee, FL, April 7-10 1997. AIAA 97-1053.

[35] Haftka R.T. Gangadharan, S.N. and Y.I. Fiocca. Variable-complexity-modeling structural optimization using response surface methodology. In *36th AIAA/ASME/ASCE/AHS/ASC Structures, Structural Dyanmics, and Materials Conference*, New Orleans, LA, April 10-12 1995. AIAA-95-1164.

[36] Unger E.R. Mason W.H. Grossman B. Hutchison, M.G. and R.T. Haftka. Variable-complexity aerodynamic optimization of a high-speed civil transport wing. *Journal of Aircraft*, 31(1):110–116, January-February 1994.

[37] Narducci R. Burgee S. Grossman B. Mason W.H. Giunta, A.A. and L.T. Watson. Variable-complexity response surface aerodynamic design of an hsct wing. In *13th AIAA Applied Aerodynamics Conference*, San Diego, CA, June 19-22 1995. AIAA-95-1886.

[38] Balabanov V. Burgee S.L. Giunta A.A. Grossman B. Mason W.H. Kaufman, M. and L.T. Watson. Variable-complexity response surface approximations for wing structural weight in hsct design. In *34th Aerospace Sciences Meeting and Exhibit*, Reno, NV, January 15-18 1996. AIAA-96-0089.

[39] Orth R.C. Billig, F.S. and M. Lasky. A unified analysis of gaseous jet penetration. *AIAA Journal*, 9(6):1048–10583, June 1971.

[40] Fuller R.F. Schetz J.A. Cox, S.K. and R.W. Walters. Vortical interactions generated by an injector array to enhance mixing in supersonic flow. In *32nd Aerospace Sciences Meeting and Exhibit*, Reno, NV, January 10-13 1994. AIAA-94-0708.

[41] D.L. Carroll. Fortran genetic algorithm driver, 1995. Version 1.6.

Vita

Captain Michael D. Payne was born to David H. and Karen W. Payne on [redacted], in [redacted]. He graduated from Penn Yan Academy in 1986 and attended Cornell University on an Air Force ROTC scholarship. In 1990, he graduated from Cornell with a Bachelor of Science degree in Mechanical & Aerospace Engineering and received a reserve commission in the United States Air Force. Captain Payne served his first tour of duty as a Management Engineering Officer at Maxwell AFB, AL. In 1993, he was transferred to Air Combat Command, Langley AFB, VA, where he was responsible for logistics modeling, simulation, and analysis for all ACC aircraft. During this tour, Captain Payne attended Auburn University and, in 1995, graduated with a Master of Aerospace Engineering degree. He entered the Air Force Institute of Technology in August, 1996, as a student of Operations Research. Captain Payne was selected for membership in Tau Beta Pi, and is currently a member of the Phi Kappa Phi and Omega Rho national honor societies. He is also a member of the American Institute of Aeronautics and Astronautics. Captain Payne and his wife, the former Melissa Eileen Cincotta, have one daughter, Ellen, and a son on the way.

Permanent Address:
[redacted]

REPORT DOCUMENTATION PAGE

Form Approved
OMB No. 0704-0188

1. AGENCY USE ONLY *(Leave blank)*	2. REPORT DATE	3. REPORT TYPE AND DATES COVERED
	March 1998	Master's Thesis

4. TITLE AND SUBTITLE
A Variable-Complexity Modeling Approach to Scramjet Combustor Design Optimization

5. FUNDING NUMBERS

6. AUTHOR(S)
Michael D. Payne, Captain, USAF

7. PERFORMING ORGANIZATION NAME(S) AND ADDRESS(ES)
Air Force Institute of Technology
Wright-Patterson AFB, OH 45433-6583

8. PERFORMING ORGANIZATION REPORT NUMBER
AFIT/GOR/ENS/98M-18

9. SPONSORING/MONITORING AGENCY NAME(S) AND ADDRESS(ES)
High Speed Systems Development (AFRL/PRSS)
1950 P Street, Bldg 18
Wright-Patterson AFB, OH 4543-7251
Attn: Dr. Mark Gruber
(937) 255-1234

10. SPONSORING/MONITORING AGENCY REPORT NUMBER

11. SUPPLEMENTARY NOTES
Dr. James Chrissis
255-6565 ext 4338
jchrissi@afit.af.mil

12a. DISTRIBUTION AVAILABILITY STATEMENT
Approved for public release; distribution unlimited

12b. DISTRIBUTION CODE

13. ABSTRACT *(Maximum 200 words)*

The analysis of fuel-air mixing in a scramjet is often accomplished either with Computational Fluid Dynamics (CFD) algorithms or through experimental research. These approaches, while accurate and reliable, are extremely expensive and thus not well-suited for use with conventional design optimization methods. In this investigation, Variable-Complexity Modeling (VCM) is used to significantly reduce the number of complex, expensive analyses required to optimize the design of a scramjet fuel injection array. A design problem formulation for a lateral transverse injection array is developed and a VCM approach to design optimization is conducted in two stages. Initially, a simplified analysis model is used to provide relatively inexpensive predictions of design fuel-air mixing characteristics. A parametric analysis is conducted to explore the design region, and a preliminary optimal design is found using both Sequential Quadratic Programming and a Genetic Algorithm. In the second stage, response surface methodology is supplemented with preliminary stage information to minimize the number of expensive analyses required to finalize the design. It is shown that only 25 design evaluations are required to develop a near-optimal design.

14. SUBJECT TERMS
Scramjet, Transverse Injection, Optimization, Sequential Quadratic Programming, Genetic Algorithm, Response Surface Methodology, Variable-Complexity Modeling

15. NUMBER OF PAGES
90

16. PRICE CODE

17. SECURITY CLASSIFICATION OF REPORT	18. SECURITY CLASSIFICATION OF THIS PAGE	19. SECURITY CLASSIFICATION OF ABSTRACT	20. LIMITATION OF ABSTRACT
Unlimited	Unlimited	Unlimited	UL